

# Response of a strongly interacting spin-orbit coupling system to a Zeeman field

Fadi Sun and Jinwu Ye

*Institute for Quantum Science and Engineering, Shenzhen 518055, China*

*Department of Physics and Astronomy, Mississippi State University, MS, 39762, USA*

(Dated: November 24, 2020)

A strongly spin-orbital coupled systems could be in a magnetic ordered phase at zero field. However, a Zeeman field could drive it into different quantum or topological phases. In a previous work, by a microscopic spin wave expansion, we study the response to a longitudinal Zeeman field of strongly interacting spinor atoms with a 2 dimensional (2d) anisotropic Rashba type of spin orbital coupling (SOC) in a square lattice. There is a special spin-orbital couple  $U(1)_{soc}$  along this anisotropic line. We find the interplay between the Zeeman field and the SOC leads to rich and novel classes of quantum commensurate (C-) and in-commensurate (IC-) phases, exotic excitations and novel quantum phase transitions. These phases include the collinear gapped Z-x at low Zeeman field, collinear gapped Z-FM at high Zeeman field, gapless co-planar canted phase at low SOC and non-coplanar IC-SkX at large SOC in intermediate Zeeman fields. In this work, starting from general symmetry principle, we construct various effective actions to study all these quantum phases and phase transitions which take different forms depending on the condensation momenta are commensurate or in-commensurate. We not only recover all these quantum phases and their excitations achieved by the microscopic calculations, but also discover several novel classes of quantum phase transitions with dynamic exponents  $z = 1, z = 2$  and anisotropic ones ( $z_x = 3/2, z_y = 3$ ) respectively. We determine the relations between the quantum spin and the order parameters of the effective actions which display rich spin-orbital structures. We find a new type of dangerously irrelevant operator we name type-II, in distinction from the known one we name type-I. We explore a new phenomena called order parameter fractionization where one complex order parameter split into two which is different than quantum spin fractionization into a spinon and a  $Z_2$  flux. Finite temperature transitions are presented. The dynamic spin-spin correlation functions are evaluated. The cases with the  $U(1)_{soc}$  symmetry explicitly broken are briefly discussed. In view of recent impressive experimental advances in generating 2d SOC for cold atoms in optical lattices, these new many-body phenomena can be explored in the near future cold atom experiments. Implications to various SOC materials such as MnSi,  $\text{Fe}_{0.5}\text{Co}_{0.5}\text{Si}$ , especially 4d Kitaev materials  $\alpha\text{-RuCl}_3$  in a Zeeman field are outlined.

## I. INTRODUCTION

During the last decade, the investigation and control of spin-orbital coupling (SOC) have become the subjects of intensive research in both condensed matter and cold atom systems after the discovery of the topological insulators [1, 2]. In the condensed matter side, there are increasing number of new quantum materials with significant SOC, including several new 4d or 5d transition metal oxides and heterostructures of transition metal systems [3, 4]. In the cold atom side, several groups worldwide [5–7] have also successfully generated a 1D (SOC) to neutral atoms. However, one of the main limitations to extend 1D SOC to a 2D SOC is the associated heating rates. Recently, there are also some advances [8–12] to overcome this difficulty in generating 2D Rashba SOC for cold atoms in both continuum and optical lattices and also in a Zeeman field. In view of these recent experimental advances, it becomes topical and important to investigate what would be new phenomena due to the interplay among strong interactions, SOC and a Zeeman field in both cold atoms and condensed matter systems.

In [13], we studied interacting spinor bosons at integer fillings loaded in a square optical lattice in the presence of non-Abelian gauge fields, in the strong coupling limit, it leads to the spin  $S = N/2$  Rotated Ferromagnetic Heisenberg model (RFHM) ( Eq.1 with  $\vec{H} = 0$  ) which is a new class of quantum spin models to describe quantum magnetisms in cold atom systems or some materials with strong SOC. Along the anisotropic line ( $\alpha = \pi/2, 0 < \beta < \pi/2$ ) of the 2d SOC, there is an exact  $U(1)_{soc}$  symmetry. We identified a new spin-orbital entangled commensurate ground state: the Y-x state. It supports not only commensurate magnons ( $C_0, C_\pi$ ), but also a new gapped elementary excitation: in-commensurate magnon ( IC ). The C-IC magnons may become the seeds to drive possible new classes of quantum C-IC transitions under various external probes. In [14], we explored the dramatic effects of an external longitudinal Zeeman field  $H$  applied to the RFHM Eq.1 along the anisotropic SOC line ( $\alpha = \pi/2, 0 < \beta < \pi/2$ ) which keeps the  $U(1)_{soc}$  symmetry. We find that the interplay among the strong interactions, SOC and the Zeeman field leads to a whole new classes of magnetic phenomena in quantum phases ( especially the non-coplanar incommensurate Skyrmion crystals (IC-SkX) ), excitation spectra ( especially inside the IC-SkX ), quantum phase transitions ( especially the quantum Commensurate to incommensurate (C-IC) transitions ), which have wide and important applications in both cold atoms and various materials with SOC. Our main results are summarized in Fig.1. Particularly, we point out

that any spin  $S = N/2$  of the RFHM can be simply achieved by tuning the number of atoms  $N$  per site, the critical temperatures of all the phases  $T_c/J \sim 2S = N$  at 2 dimension can be easily increased above that reachable by the current cold atom cooling techniques. In [15], we studied the response to a transverse field of the RFHM Eq.1 along the anisotropic SOC line ( $\alpha = \pi/2, 0 < \beta < \pi/2$ ). Because the transverse field breaks the  $U(1)_{soc}$  symmetry, so the response is quite different than that in a longitudinal field. However, the approach used in [13–15] is exact symmetry analysis plus microscopic spin wave expansion, so can not be used to study the nature of all these quantum phase transitions. A complete independent symmetry based phenomenological effective action is needed to achieve this goal.

In this work, starting from symmetry principle, we construct various effective actions to study all these quantum phases and phase transitions in Fig.1. We recover all these quantum phases and their excitations discovered by the microscopic calculations in [13–15], most importantly, explore the nature of all the quantum phase transitions, therefore provide deep insights into the global phase diagram in Fig.1. Furthermore, we find a new type of dangerously irrelevant operator: it is irrelevant near the QCP, but marginal in the symmetry breaking ground state. So it does not change the ground state, but changes its excitation spectrum to an exotic form. This is in sharp contrast to the known dangerously irrelevant operator [16–18, 22]: it is irrelevant near the QCP, but relevant in the symmetry breaking ground state. So it change both the ground state and the excitation spectrum. We name the known one and the new one as Type-I and Type-II dangerously irrelevant operator respectively. The Z-x state to the IC-SkX transition at  $h = h_{c1}$  is in the same universality class as the  $z = 2$  SF-Mott transition with  $U(1)_{soc}$  symmetry. There is also a type-II dangerously irrelevant operator which leads to one exotic Goldstone mode inside the IC-SkX phase near  $h_{c1}$ . However, at the mirror symmetry point, the Type-II dangerously irrelevant operator is absent, the exotic Goldstone mode recovers to the conventional one. The FM state to the IC-SkX transition at  $h = h_{c2}$  in the middle range  $\beta_1 < \beta < \beta_2 = \pi/2 - \beta_1$  of SOC is in the same universality class as a  $z = 2$  two-component SF-Mott transition in the Ising limit with a  $U(1)_{soc} \times U(1)_{ic}$  symmetry, the extra  $U(1)_{ic}$  symmetry comes from the magnon condensation at two in-commensurate momenta. There are two type-II dangerously irrelevant operators which lead to one exotic gapless Goldstone mode and one gapped exotic roton mode inside the IC-SkX phase near  $h_{c2}$ . However, at the mirror symmetry point, the two Type-II dangerously irrelevant operators are absent, there is a quartic Umklapp term which breaks the extra  $U(1)_{ic}$  symmetry, the exotic Goldstone and roton mode recover to the conventional ones. The FM state to the canted phase transition at  $h = h_{c2}$  in the left ( or ) right range  $0 < \beta < \beta_1$  ( or  $\beta_2 < \beta < \pi/2$  ) of SOC is in the same universality class of  $z = 1$  boosted SF-Mott transition with  $U(1)_{soc}$  symmetry. It is the boost due to the SOC which leads to one exotic Goldstone mode and one exotic Higgs mode inside the canted phase. However, at the  $\beta = 0$  Abelian point which maps to a FM in the presence of a staggered Zeeman field along  $x$ - axis, the boost is absent, the transition reduces to the  $z = 1$  3d XY class, the exotic Goldstone and Higgs modes recover to the conventional ones. Inside the canted phase, as the SOC increases at a fixed Zeeman field, the transition from the canted phase to the IC-SkX phase is a novel class of quantum Lifshitz transition with the anisotropic dynamic exponent ( $z_x = 3/2, z_y = 3$ ). There is an order parameter fractionization from one complex order parameter to TWO from the left ( canted to IC-SkX ), or equivalently, an order parameter reduction from TWO complex order parameters to one from the right ( IC-SkX to canted ). Finite temperature transitions above all these quantum phases and QPTs are presented. We also examine carefully the relations between the quantum spins and the order parameters which involve linearly the unitary transformation below  $h_{c1}$  and Bogliubov transformation above  $h_{c2}$ . We also show that these relations still hold phenomenologically when  $h_{c1} < h < h_{c2}$  inside the IC-SkX phase, despite the two transformations are not defined anymore in the range of the Zeeman field. The dynamic spin-spin correlation functions are evaluated by using these relations. Transverse fields which explicitly break the  $U(1)_{soc}$  symmetry are also discussed. In view of recent impressive experimental advances in generating 2d SOC for cold atoms in optical lattices, these new many-body phenomena can be explored in the current and near future cold atom experiments. Some implications to various SOC materials such as MnSi, Fe<sub>0.5</sub>Co<sub>0.5</sub>Si with a strong Dzyaloshinskii-Moriya (DM) interaction, especially the recently discovered 4d Kitaev materials  $\alpha - RuCl_3$  in a Zeeman field are discussed. Some future perspectives are outlined.

Despite there are many previous works on the Boson-Einstein condensation (BEC) of bosons, there are very little works on magnon condensation in a quantum magnet which is very much different from the BEC. There is a previous work [19] phenomenologically assuming the magnon condensation with a  $U(1)_s$  spin-rotation symmetry is in the same universality class as a 2d  $z = 2$  SF-Mott transition. This spin  $U(1)_s$  symmetry mimics the charge conservation symmetry of the bosons. This assumption is confirmed in appendix F. Our work here in the longitudinal field also has one  $U(1)_{soc}$  symmetry, however, it is a spin-orbital coupled  $U(1)_{soc}$  symmetry, so very much different than the spin  $U(1)_s$  symmetry. Indeed, as demonstrated in the main text and summarized above, the magnon condensation with SOC is also dramatically different than that without SOC [19]. Of course, the BEC of spinor bosons with SOC [20–24] is also dramatically different than that without SOC.

Due to the SOC, the response dramatically depends on the orientation of the magnetic field, in the main text, we focus on the longitudinal field, in the appendix E, we will discuss the two transverse fields.

The spin  $S = N/2$  Rotated Ferromagnetic Heisenberg model at a generic SOC parameters  $(\alpha, \beta)$  in a Zeeman field

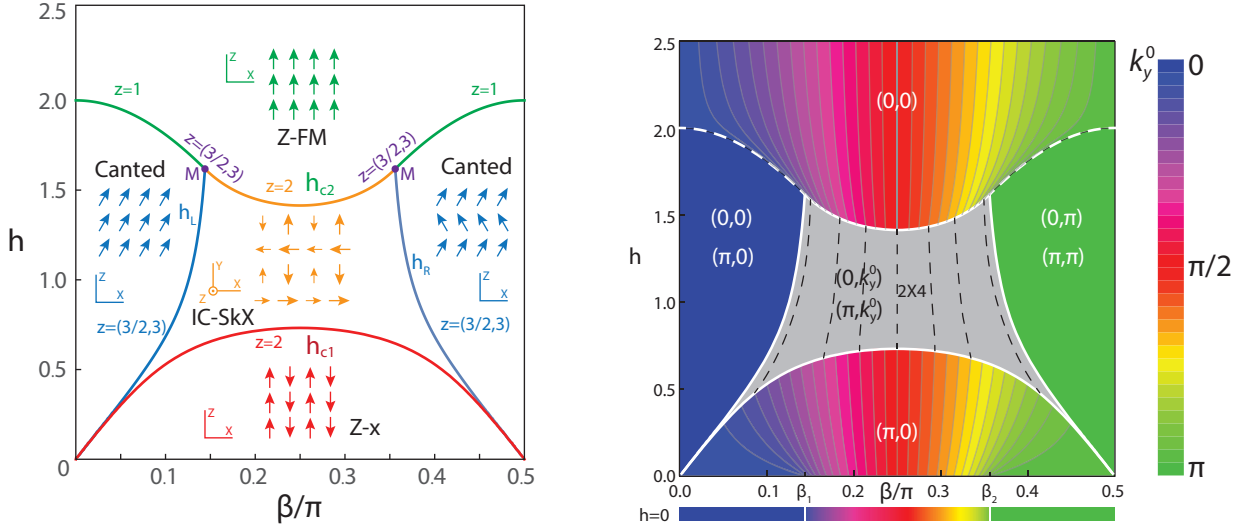


FIG. 1. Quantum Phases and phase transitions of RFHM in a longitudinal Zeeman field Eq.(2) achieved by the combination of the microscopic SWE [14] and the effective actions here. (a) Below  $h_{c1}$  is the spin-orbital correlated (collinear) Z-x state. Above  $h_{c2}$  is the (collinear) Z-FM state. Note the three different pieces of  $h_{c2}$ . On the left,  $h_L$  is one canted (co-planar) state. On the right,  $h_R$  is another canted (co-planar) state. Surrounded by the four commensurate phases is the in-commensurate Skyrion crystal (non-coplanar) phase (IC-SkX) with non-vanishing Skyrion density. At  $\beta = \pi/4$ , the IC-SkX reduces to a  $2 \times 4$  commensurate SkX where only the spins (with two different lengths) in the  $XY$  plane are shown. There is a multi-critical ( M ) point where the ( collinear ) Z-FM, the ( co-planar ) canted phase and the ( non-co-planar ) IC-SkX phase meet. The phases on the left  $\beta < \pi/4$  are related to the right  $\beta > \pi/4$  by the Mirror transformation. The center  $\beta = \pi/4$  respects the Mirror symmetry. The quantum phase transitions between (among) these phases with the dynamic exponents  $z = 1$ ,  $z = 2$  and the anisotropic one ( $z_x = 3/2$ ,  $z_y = 3$ ), especially the three different classes of quantum commensurate to In-commensurate transitions are discussed in the text. (b) The orbital ordering wavevectors of the two collinear, two coplanar and the non-coplanar phases. The constant contour plot of the minima  $(0, k_y^0)$  of the C-IC magnons in the Z-x state at  $h < h_{c1}$  and Z-FM state at  $h > h_{c2}$ , connected by the orbital ordering wavevectors ( dashed line ) inside the IC-SkX. There are one C-C transition from the canted phase to the Z-FM at  $(h_{c2}, 0 < \beta < \beta_1)$  with the dynamic exponent  $z = 1$ . There are three different kinds of C-IC transitions at  $h_{c1}$ ,  $(h_{c2}, \beta_1 < \beta < \beta_2)$  and  $h_L$  ( or  $h_R$  ) from the IC-SkX to the Z-x, Z-FM and canted phase with the dynamic exponents  $z = 2$ ,  $z = 2$  and ( $z_x = 3/2$ ,  $z_y = 3$ ) respectively. For the two transverse fields, see appendix E.

$\vec{H}$  along any direction is [13]:

$$\mathcal{H}_{RH} = -J \sum_i [\mathbf{S}_i R(\hat{x}, 2\alpha) \mathbf{S}_{i+\hat{x}} + \mathbf{S}_i R(\hat{y}, 2\beta) \mathbf{S}_{i+\hat{y}}] - \vec{H} \cdot \sum_i \vec{S}_i \quad (1)$$

where the  $R(\hat{x}, 2\alpha)$ ,  $R(\hat{y}, 2\beta)$  are two  $SO(3)$  rotation matrices around the  $\hat{x}, \hat{y}$  spin axis by angle  $2\alpha, 2\beta$  putting along the two bonds  $x, y$  respectively,  $H$  is the Zeeman field which could be induced by the Raman laser in the cold atom set-ups [8–12].

Following [14], we focus on studying the phenomena along the line ( $\alpha = \pi/2, 0 < \beta < \pi/2$ ) and in the Zeeman field along the longitudinal  $y$  direction. After rotating spin  $Y$  axis to  $Z$  axis by the global rotation  $R(\hat{x}, \pi/2)$ , the Hamiltonian Eqn.1 along the line ( $\alpha = \pi/2, 0 < \beta < \pi/2$ ) in the  $H$  field along  $y$  direction can be written as:

$$\mathcal{H} = -J \sum_i \left[ \frac{1}{2} (S_i^+ S_{i+x}^+ + S_i^- S_{i+x}^-) - S_i^z S_{i+x}^z + \frac{1}{2} (e^{i2\beta} S_i^+ S_{i+y}^- + e^{-i2\beta} S_i^- S_{i+y}^+) + S_i^z S_{i+y}^z \right] - H \sum_i S_i^z \quad (2)$$

where the Zeeman field  $H$  is along the  $z$  direction after the global rotation.

The symmetry of the Hamiltonian Eq.2 is generated by [25]

1. Translation by one lattice site in  $x$  or  $y$  direction:  $\mathcal{T}_x : S_i \rightarrow S_{i+\hat{x}}$  and  $\mathcal{T}_y : S_i \rightarrow S_{i+\hat{y}}$ .
2. Space reflection with respect to  $y$  axis:  $\mathcal{I}_y : S_i \rightarrow S_{\bar{i}}$ , where  $i = (i_x, i_y)$  and  $\bar{i} = (-i_x, i_y)$ .
3. Spin reflection symmetry:  $\mathcal{P}_z : S_i \rightarrow R_z(\pi) S_i$
4. Spin-orbital  $U(1)$  spin-rotation:  $\mathcal{R} : S_i \rightarrow R_z((-1)^{i_x} \phi) S_i$
5. Spin-orbital reflection:  $\mathcal{T} \circ \mathcal{I}_x \circ \mathcal{P}_x$  and  $\mathcal{T} \circ \mathcal{I}_x \circ \mathcal{P}_y$ .

6. \* Enlarged mirror symmetry:  $\mathcal{T} \circ \mathcal{M}$ , where  $\mathcal{M} : S_i \rightarrow R_x(\pi)R_z(i_y\pi)S_i$ . It maps Hamiltonian soc parameter  $\beta \rightarrow \pi/2 - \beta$ .  $\mathcal{T} \circ \mathcal{M} : (S_i^x, S_i^y, S_i^z) \rightarrow (-(-1)^{i_y}S_i^x, (-1)^{i_y}S_i^y, S_i^z)$

Some of these symmetries are broken in the Z-x, canted and IC-SkX phases, but preserved in the Z-FM state. They are quite crucial to construct the corresponding effective actions to be presented in the following.

We will take  $2SJ$  as the energy unit, so all the physical quantities such as the Zeeman field  $H$ , the magnon dispersion  $\omega_k$  and the gap  $\Delta$  will be dimensionless after taking their ratios over  $2SJ$ . We will first focus on the left half of Fig.1 with  $0 < \beta < \pi/4$ , then study the right half using the Mirror transformation  $\mathcal{M}$ . The mirror center  $\beta = \pi/4$  respects the Mirror symmetry.

## II. QUANTUM PHASE TRANSITION AT THE LOWER CRITICAL FIELD $h_{c1}$

The spin wave expansion (SWE) in the Z-x state below  $h_{c1}$  was performed in [14] and reviewed in the appendix A. Dropping the higher branch  $\alpha_{\mathbf{k}}$  in Eq.B5, it is the  $\beta_{\mathbf{k}}$  magnon condensation at  $\mathbf{K}_0 = (0, k_0)$  which leads to the QPT from the Z-x state to the IC-SkX at  $h_{c1}$  in the whole range of  $0 < \beta < \pi/2$ . The order parameter takes the form:

$$\langle \beta_{\mathbf{k}} \rangle = \psi \delta_{\mathbf{k}, \mathbf{K}_0}, \quad \langle \alpha_{\mathbf{k}} \rangle = 0 \quad (3)$$

where  $\mathbf{K}_0 = (0, k_0)$  and  $\psi$  is a complex order parameter.

One must use the unitary transformation Eq.(B4) to establish the connection between the transverse quantum spin and the order parameter:

$$S_{A,i}^+ = \sqrt{2S} \langle a_i \rangle = c\psi e^{ik_0 i_y} \quad S_{B,j}^- = \sqrt{2S} \langle b_j \rangle = s\psi e^{ik_0 j_y} \quad (4)$$

where  $c = c_{\mathbf{K}_0}$  and  $s = s_{\mathbf{K}_0}$  are evaluated at  $\mathbf{K}_0 = (0, k_0)$ . It is easy to see that  $\langle \psi \rangle = 0$  at  $h < h_{c1}$  gives back to the Z-x state.  $\langle \psi \rangle \neq 0$  at  $h < h_{c1}$  leads to the IC-SkX state.

The Z-x state spontaneously break the translation along the  $x$ - direction by one lattice site to two lattice site, i.e.  $\mathcal{T}_x \rightarrow (\mathcal{T}_x)^2$ , but still keeps all the other symmetries of the Hamiltonian listed in the introduction. After incorporating this fact, one can study how  $\psi$  transform under the symmetries of the Hamiltonian:

1. Translation:  $(\mathcal{T}_x)^2 : \psi(x, y) \rightarrow \psi(x, y)$  and  $\mathcal{T}_y : \psi(x, y) \rightarrow e^{ik_0} \psi(x, y)$ ;
2. Space reflection:  $\mathcal{I}_y : \psi(x, y) \rightarrow \psi(-x, y)$ ;
3. Spin reflection:  $\mathcal{P}_z : \psi(x, y) \rightarrow -\psi(x, y)$ ;
4. Spin-orbital  $U(1)_{soc}$  rotation:  $\mathcal{R} : \psi(x, y) \rightarrow e^{i\phi_0} \psi(x, y)$ ;
5. Spin-orbital reflection:  $\mathcal{T} \circ \mathcal{I}_x \circ \mathcal{P}_x : \psi(x, y) \rightarrow -\psi^*(x, -y)$  and  $\mathcal{T} \circ \mathcal{I}_x \circ \mathcal{P}_y : \psi(x, y) \rightarrow \psi^*(x, -y)$ ;
6. Enlarged mirror symmetry at  $\beta = \pi/4$ :  $\mathcal{T} \circ \mathcal{M} : \psi(x, y) \rightarrow -\psi^*(x, y)$ .

Combining the mirror symmetry at  $\beta = \pi/4$  with the spin-orbital reflection leads to the fact that  $\mathcal{I}_x \circ \mathcal{P}_x \circ \mathcal{M}$  maps  $\psi(x, y)$  to  $\psi(x, -y)$  for  $\beta = \pi/4$ . It dictates an odd derivative in  $\partial_y$  is absent at  $\beta = \pi/4$ , but may appear when away from  $\beta = \pi/4$ . The  $\mathcal{I}_y$  at a general  $\beta$  dictates an odd derivative in  $\partial_x$  is always absent.

The above symmetry analysis suggests the following effective action in the continuum limit with the dynamic exponent  $z = 2$

$$\mathcal{S}_{\text{low}} = \int d\tau d^2r [\psi^* \partial_\tau \psi + v_x^2 |\partial_x \psi|^2 + v_y^2 |\partial_y \psi|^2 - \mu |\psi|^2 + U |\psi|^4 + iV |\psi|^2 \psi^* \partial_y \psi + \dots] \quad (5)$$

Our microscopic calculation shows that  $\mu = h - h_{c1}$ ,  $U > 0$  and  $V \propto \sin(2k_0)$  which vanishes at  $\beta = \pi/4$  dictated by the mirror symmetry. Due to the factoring of  $e^{ik_0 i_y}$  in Eq.4, the odd derivative in  $\partial_y$  term first appears in the interaction  $V$  term.

### A. The spin-orbital order of the ground state

At mean field level, we can substitute  $\psi = \psi_0 = \sqrt{\rho_0}e^{i\phi_0}$  to the effective action Eq.5 and obtain

$$S_0 = -\mu\rho_0 + U\rho_0^2 \quad (6)$$

When  $\mu < 0$  at  $h < h_{c1}$ , it is in the Z-x state with  $\langle\psi\rangle = 0$ . When  $\mu > 0$  at  $h > h_{c1}$ , it is in the IC-SkX state with  $\langle\psi\rangle = \sqrt{\rho_0}e^{i\phi_0}$  where  $\rho_0 = \sqrt{\mu/2U}$  and  $\phi_0$  is a arbitrary angle due to  $U(1)_{\text{soc}}$  symmetry.

Combining Eq.4 with the constraint  $|\mathbf{S}_i|^2 = S^2$ , one obtain the spin-orbital order of the IC-SkX phase above  $h_{c1}$ :

$$\begin{aligned} S_i^+ &= (\sqrt{\rho_0}/2)[c + s + (-1)^{i_x}(c - s)]e^{(-1)^{i_x}i(k_0i_y + \phi_0)} \\ S_i^z &= [\sqrt{S^2 - \rho_0c^2} - \sqrt{S^2 - \rho_0s^2} + (-1)^{i_x}(\sqrt{S^2 - \rho_0c^2} + \sqrt{S^2 - \rho_0s^2})] \end{aligned} \quad (7)$$

where the sign  $\pm\sqrt{S^2 - |S^+|^2}$  is chosen such that  $S_i^z$  reproduce the Z-x order when  $\rho_0 \rightarrow 0$ . It leads to the spin-orbital order in the IC-SkX phase when  $h < h_*$  which is the fixed point in IC-SkX phase where one of the two sublattices  $S_i^z = 0$ .

One can also calculate

$$\lim_{h \rightarrow h_{c1}^-} \frac{|S_A^+|}{|S_B^+|} = \lim_{h \rightarrow h_{c1}^-} \frac{c}{s} = [2 - \cos 2\beta \cos k_0 - \sqrt{(2 - \cos 2\beta \cos k_0)^2 - 1}] \quad (8)$$

which indeed matches the ratio  $|S_A^+|/|S_B^+|$  calculated by SWE from  $h_{c1}^+$  shown in Eq.C6.

It is important to stress that the quantum spin in Eq.7 is linearly related to the magnon operator, in contrast to many other cases where the quantum spin is quadratically represented in terms of spinon operators. Amazingly, despite the unitary matrix element  $c$  and  $s$  are only well defined below  $h < h_{c1}$ . We can still take them as two phenomenological parameters in Eq.7 inside the IC-SkX above  $h > h_{c1}$ . It matches the microscopic SWE calculation in [14].

### B. Excitation spectrum: exotic Goldstone mode

When  $\mu < 0$ ,  $\langle\psi\rangle = 0$  inside the Z-x state, expanding the effective action upto second order in  $\psi$  leads to:

$$S_2 = \int d\tau d^2r [\psi^* \partial_\tau \psi + v_x^2 |\partial_x \psi|^2 + v_y^2 |\partial_y \psi|^2 - \mu |\psi|^2] \quad (9)$$

which leads to the gapped excitation spectrum

$$\omega_{\mathbf{k}} = \sqrt{-\mu + v_x^2 k_x^2 + v_y^2 k_y^2} \quad (10)$$

which matches the results achieved by the microscopic SWE calculation in [14].

When  $\mu > 0$ ,  $\langle\psi\rangle = \sqrt{\rho_0}e^{i\phi_0}$  inside the IC-SkX state, by writing the fluctuations in the polar coordinate  $\psi = \sqrt{\rho_0 + \delta\rho}e^{i(\phi_0 + \delta\phi)}$ , one can expand the action up to the second order in the fluctuations:

$$S_2 = \int d\tau d^2r \left( i\delta\rho \partial_\tau \delta\phi + \frac{1}{4\rho_0} [v_x^2 (\partial_y \delta\rho)^2 + v_y^2 (\partial_y \delta\rho)^2] + \rho_0 [v_x^2 (\partial_x \delta\phi)^2 + v_y^2 (\partial_y \delta\phi)^2] + U(\delta\rho)^2 - V\rho_0 \delta\rho \partial_y \delta\phi \right) \quad (11)$$

where one can see the odd derivative in  $\partial_y$  term turns into a quadratic term inside the IC-SkX phase.

Integrating out  $\delta\rho$  leads to

$$S_2 = \int d\tau d^2r \left( \frac{1}{4U} [(\partial_\tau - i\rho_0 V \partial_y) \phi]^2 + \rho_0 [v_x^2 (\partial_x \delta\phi)^2 + v_y^2 (\partial_y \delta\phi)^2] \right) \quad (12)$$

where one can see the odd derivative in  $\partial_y$  term sneaks into  $\partial_\tau$  term inside the IC-SkX phase and behaves like a boost term to be discussed in Sec.IV. It leads to the exotic Goldstone mode due to the  $U(1)_{\text{soc}}$  symmetry breaking:

$$\omega_{\mathbf{k}} = \sqrt{4U\rho_0(v_x^2 k_x^2 + v_y^2 k_y^2)} - V\rho_0 k_y \quad (13)$$

which recovers the conventional Goldstone mode at the mirror symmetric point  $\beta = \pi/4$ .

### C. QPT: Type-II dangerously irrelevant operators away from the mirror symmetric point

At the mirror symmetric point  $\beta = \pi/4$ ,  $V = 0$ , so the effective action Eq.5 is in the same universality class as the  $z = 2$  zero density SF-Mott transition where the interaction  $U$  term is marginally irrelevant. When away from the mirror symmetric point, the  $V$  term moves in. However, simple power counting shows that it is irrelevant near the  $z = 2$  zero density SF-Mott QCP. However, inside the IC-SkX phase, as shown in Eq.13, it modifies the spectrum of the Goldstone mode by an extra linear term, so it is marginal and plays a crucial role inside the phase. This is sharp contrast to the well known dangerously irrelevant operator which is irrelevant near the QCP, but relevant inside the phase and changes the ground state. We call this new type of dangerously irrelevant operator Type -II, while the known one as Type-I. For example, the Type-I appears and leads to the  $N = 2$  XY-AFM phase presented in [22].

So the universality class for the QPT at  $h_{c1}$  is nothing but the  $z = 2$  2d SF-Mott transition at the mirror symmetric point, plus a Type-II dangerous irrelevant operator away from it.

### III. QUANTUM PHASE TRANSITION AT THE UPPER CRITICAL FIELD $h_{c2}$ IN THE MIDDLE RANGE $\beta_1 < \beta < \beta_2$ .

The SWE in the FM state above  $h_{c2}$  was also performed in [14] and reviewed in appendix B2. It is the  $\alpha_{\mathbf{k}}$  magnon condensation in Eq.B12 which leads to the QPT from the FM state to the IC-SkX at  $h_{c2}$  in the middle range  $\beta_1 < \beta < \beta_2$ . The order parameter takes the form:

$$\langle \alpha_{\mathbf{k}} \rangle = \psi_1 \delta_{\mathbf{k}, \mathbf{K}_1} + \psi_2 \delta_{\mathbf{k}, \mathbf{K}_2} \quad (14)$$

where  $\mathbf{K}_1 = (0, k_0)$ ,  $\mathbf{K}_2 = (\pi, k_0)$  and  $\psi_1, \psi_2$  are the two complex order parameters.

One must use the Bogoliubov transformation Eq.(B10) to establish the connection between the transverse quantum spin and the two complex order parameters:

$$\langle S_i^+ \rangle \propto u[\psi_1 + (-1)^{i_x} \psi_2] e^{ik_0 i_y} + v[\psi_1^* - (-1)^{i_x} \psi_2^*] e^{-ik_0 i_y} \quad (15)$$

where  $u = u_{\mathbf{K}_1} = u_{\mathbf{K}_2}$  and  $v = v_{\mathbf{K}_1} = -v_{\mathbf{K}_2}$ .

Because the Z-x state breaks no symmetry of the Hamiltonian, so one can study how  $\psi_1$  and  $\psi_2$  transform under the symmetries of the Hamiltonian listed in the Introduction:

1. Translation:  $\mathcal{T}_x : (\psi_1, \psi_2)(x, y) \rightarrow (\psi_1, -\psi_2)(x, y)$  and  $\mathcal{T}_y : (\psi_1, \psi_2)(x, y) \rightarrow (e^{ik_0} \psi_1, e^{ik_0} \psi_2)(x, y)$ ;
2. Space reflection:  $\mathcal{I}_y : (\psi_1, \psi_2)(x, y) \rightarrow (\psi_1, \psi_2)(-x, y)$ ;
3. Spin reflection:  $\mathcal{P}_z : (\psi_1, \psi_2)(x, y) \rightarrow (-\psi_1, -\psi_2)(x, y)$ ;
4. Spin-orbital U(1) rotation:  $\mathcal{R} : (\psi_1, \psi_2)(x, y) \rightarrow (\psi_1 \cos \phi + i\psi_2 \sin \phi, \psi_2 \cos \phi + i\psi_1 \sin \phi)(x, y)$ ;
5. Spin-orbital reflection:  $\mathcal{T} \circ \mathcal{I}_x \circ \mathcal{P}_x : (\psi_1, \psi_2)(x, y) \rightarrow (-\psi_1^*, -\psi_2^*)(x, -y)$   
and  $\mathcal{T} \circ \mathcal{I}_x \circ \mathcal{P}_y : (\psi_1, \psi_2)(x, y) \rightarrow (\psi_1^*, \psi_2^*)(x, -y)$ ;
6. Enlarged mirror symmetry at  $\beta = \pi/4$ :  $\mathcal{T} \circ \mathcal{M} : (\psi_1, \psi_2)(x, y) \rightarrow (-\psi_1^*, -\psi_2^*)(x, y)$ .

where the notation  $(\psi_1, \psi_2)(x, y)$  means  $(\psi_1(x, y), \psi_2(x, y))$ .

Combining the mirror symmetry at  $\beta = \pi/4$  with the spin-orbital reflection leads to the fact that  $\mathcal{I}_x \circ \mathcal{P}_x \circ \mathcal{M}$  maps  $(\psi_1, \psi_2)(x, y)$  to  $(\psi_1, \psi_2)(x, -y)$  for  $\beta = \pi/4$ . It dictates an odd derivative in  $\partial_y$  is absent at  $\beta = \pi/4$ , but may appear when away from  $\beta = \pi/4$ . The  $\mathcal{I}_y$  at a general  $\beta$  dictates an odd derivative in  $\partial_x$  is always absent. The above symmetry analysis suggests the following two-component effective action with the dynamic exponent  $z = 2$  in the continuum limit,

$$\begin{aligned} \mathcal{S}_{12} = \int d\tau d^2r [ & \sum_{\alpha=1,2} (\psi_\alpha^* \partial_\tau \psi_\alpha + v_x^2 |\partial_x \psi_\alpha|^2 + v_y^2 |\partial_y \psi_\alpha|^2) - \mu(|\psi_1|^2 + |\psi_2|^2) + U(|\psi_1|^2 + |\psi_2|^2)^2 - A(\psi_1 \psi_2^* + \psi_1^* \psi_2)^2 \\ & + iV_1(|\psi_1|^2 + |\psi_2|^2)(\psi_1^* \partial_y \psi_1 + \psi_2^* \partial_y \psi_2) + iV_2(\psi_1 \psi_2^* + \psi_1^* \psi_2)(\psi_1 \partial_y \psi_2^* + \psi_1^* \partial_y \psi_2) ] \end{aligned} \quad (16)$$

Our microscopic calculation shows that  $\mu = h_{c2} - h$ ,  $U = h(u^2 + v^2)^2 + 2(1 + h) > A = (4 + h) > 0$ . Furthermore,  $V_1, V_2 \propto \sin(2k_0)$ , both of which vanish at  $\beta = \pi/4$  dictated by the Mirror symmetry. Due to the factoring out of  $e^{\pm ik_0 i_y}$  in Eq.15, the odd derivative in  $\partial_y$  term first appears in the interaction  $V_1, V_2$  terms.

In fact, as suggested by Eq.15, the physics may become more transparent in the new basis:

$$\psi_+ = (\psi_1 + \psi_2)/\sqrt{2}, \quad \psi_- = (\psi_1 - \psi_2)/\sqrt{2} \quad (17)$$

where the above effective action becomes [46]

$$\begin{aligned} \mathcal{S}_\pm = \int d\tau d^2r [ & \sum_{\alpha=+,-} (\psi_\alpha^* \partial_\tau \psi_\alpha + v_x^2 |\partial_x \psi_\alpha|^2 + v_y^2 |\partial_y \psi_\alpha|^2) - \mu(|\psi_+|^2 + |\psi_-|^2) + U(|\psi_+|^2 + |\psi_-|^2)^2 - A(|\psi_+|^2 - |\psi_-|^2)^2 \\ & + iV_1(|\psi_+|^2 + |\psi_-|^2)(\psi_+^* \partial_y \psi_+ + \psi_-^* \partial_y \psi_-) + iV_2(|\psi_+|^2 - |\psi_-|^2)(\psi_+ \partial_y \psi_-^* - \psi_- \partial_y \psi_+^*) ] \end{aligned} \quad (18)$$

which enjoys a  $U(1)_{soc} \times U(1)_{ic}$  symmetry when  $k_0/\pi$  is an irrational number. The first SOC  $U(1)_{soc}$  maps  $(\psi_+, \psi_-) \rightarrow (e^{i\phi_0} \psi_+, e^{-i\phi_0} \psi_-)$ , while the second  $U(1)_{ic}$  is generated by the whole family of  $\mathcal{T}_y^n, n = 1, 2, 3, \dots$  which maps  $(\psi_+, \psi_-) \rightarrow (e^{ik_0 n} \psi_+, e^{ik_0 n} \psi_-)$ . Because  $k_0/\pi$  is an irrational number, so  $\theta_0 = k_0 n$  becomes a continuous variable leading to a new emergent  $U(1)_{ic}$  symmetry.

However, if  $k_0/\pi = p/q$  with  $p$  and  $q$  are two coprime positive integers, then  $(\mathcal{T}_y)^{2q} = 1$  and the action should include an extra Umklapp term:

$$\begin{aligned} \mathcal{S}_{Um} = \int d\tau d^2r [ & B_q(\psi_1^2 - \psi_2^2)^q + c.c.] + [iC_q(\psi_1^2 - \psi_2^2)^{q-1}(\psi_1 \partial_y \psi_2 - \psi_2 \partial_y \psi_1) + c.c.] + \dots \} \\ = 2^q \int d\tau d^2r [ & B_q(\psi_+ \psi_-)^q + c.c.] + [iC_q(\psi_+ \psi_-)^{q-1}(\psi_+ \partial_y \psi_-) + c.c.] + \dots \} \end{aligned} \quad (19)$$

which breaks explicitly only the  $U(1)_{ic}$ , but not the  $U(1)_{soc}$  symmetry. The  $B_q, C_q$  maybe complex for  $\beta \neq \pi/4$  and  $\dots$  means high order terms with power  $2nq$  ( $n > 1$ ).

At the mirror symmetric point  $\beta = \pi/4$ ,  $k_0 = \pi/2$  with  $q = 2$ , then  $\mathcal{S}_{Um}$  is quartic order in  $\psi_{1,2}$ . So one must consider this  $B_2$  term at  $\beta = \pi/4$  where the mirror symmetry dictates  $C_2 = 0$  and also the absence of the two type-II dangerously irrelevant  $V_1, V_2$  terms.

$$\begin{aligned} \mathcal{S}_M = \int d\tau d^2r [ & \sum_{\alpha=+,-} (\psi_\alpha^* \partial_\tau \psi_\alpha + v_x^2 |\partial_x \psi_\alpha|^2 + v_y^2 |\partial_y \psi_\alpha|^2) - \mu(|\psi_+|^2 + |\psi_-|^2) + U(|\psi_+|^2 + |\psi_-|^2)^2 \\ & - A(|\psi_+|^2 - |\psi_-|^2)^2 + B_2(\psi_+ \psi_-)^2 + c.c.] \end{aligned} \quad (20)$$

In the regime  $0 \leq k_0 \leq \pi/2$  in Fig.2a,  $q \geq 2$ , so  $\mathcal{S}_{Um}$  becomes higher order when  $\beta < \pi/4$  with  $q > 2$ . Then it become highly irrelevant in the renormalization group (RG) sense, so can be dropped [28].

### A. The spin-orbital order of the ground state

The  $\psi_\pm$  basis is good for symmetry analysis see Sec.C. However, the saddle point solution ( $\langle \psi_- \rangle = 0, \langle \psi_+ \rangle \neq 0$  or ( $\langle \psi_- \rangle \neq 0, \langle \psi_+ \rangle = 0$ ) inside the IC-SkX phase, so it is not convenient to investigate quantum fluctuations in the polar coordinate [51]. Here, we get back to the  $(\psi_1, \psi_2)$  basis. At mean-field level, we can substitute  $\psi_\alpha \rightarrow \sqrt{\rho_\alpha} e^{i\phi_\alpha}, \alpha = 1, 2$  to the effective action Eq.16

$$\begin{aligned} \mathcal{S}_0 & \propto -\mu(\rho_1 + \rho_2) + U(\rho_1 + \rho_2)^2 - 4A\rho_1\rho_2 \cos^2(\phi_1 - \phi_2) \\ & = -\mu(\rho_+ + \rho_-) + U(\rho_+ + \rho_-)^2 - A(\rho_+ - \rho_-)^2 \end{aligned} \quad (21)$$

When  $\mu = h_{c2} - h < 0$ , it is in the Z-FM phase with  $\langle \psi_1 \rangle = \langle \psi_2 \rangle = 0$ . When  $\mu > 0$ , it is in the IC-SkX phase with  $\langle \psi_1 \rangle = \langle \psi_2 \rangle = \sqrt{\rho_0/2} e^{i\phi_0}$  and  $\rho_1 = \rho_2 = \rho_0/2 = \sqrt{\mu/8(U-A)}$ . It is easy to see the symmetry breaking pattern is described by the coset:

$$U(1)_{soc} \times U(1)_{ic} / [U(1)_{soc} \times U(1)_{ic}]_D \quad (22)$$

where the diagonal ( D ) means  $y \rightarrow y + n, \phi_0 \rightarrow \phi_0 - nk_y^0$  generated by  $\mathcal{T}_y^n \times \mathcal{R}(nk_y^0)$  for any integer  $n$  [26]. The coset dictates only one Goldstone mode. Note that the IC-SkX phase breaks all other symmetries of the Hamiltonian except  $\mathcal{I}_x$  and  $[U(1)_{soc} \times U(1)_{ic}]_D$ .

For the commensurate case  $k_0/\pi = p/q$ , we may also include the Umklapp contribution:

$$\mathcal{S}_0 \propto -\mu(\rho_1 + \rho_2) + U(\rho_1 + \rho_2)^2 - 4A\rho_1\rho_2 \cos^2(\phi_1 - \phi_2) + B_q[(\rho_1 e^{i2\phi_1} - \rho_2 e^{i2\phi_2})^q + c.c.] \quad (23)$$

When  $A \gg |B_q|$ , the mean field solution  $\langle \psi_1 \rangle = \langle \psi_2 \rangle = 0$  for  $\mu < 0$  and  $\langle \psi_1 \rangle = \langle \psi_2 \rangle = \sqrt{\rho_0/2}e^{i\phi_0}$  for  $\mu > 0$  still holds. This fact can be best seen in the  $(\psi_+, \psi_-)$  basis:

$$S_0 \propto -\mu(\rho_+ + \rho_-) + (U - A)(\rho_+ + \rho_-)^2 + 4\rho_+\rho_- \{A + 2B_q(4\rho_+\rho_-)^{q/2-1} \cos[q(\phi_+ + \phi_-)]\} \quad (24)$$

where  $\rho_+ + \rho_- = \rho_0$ .

When  $A > 2|B_q|\rho_0^{q-2}$ , the last term is always non-negative which ensures  $\rho_+\rho_- = 0$  in the mean field ground-state.

Combing Eq.15 with the constraint  $|\mathbf{S}_i|^2 = S^2$ , one obtain the spin-orbital order of the IC-SkX phase below  $h_{c2}$

$$\begin{aligned} S_i^+ &= \sqrt{\rho_0/2}[u + v + (-1)^{i_x}(u - v)]e^{(-1)^{i_x}i(k_0 i_y + \phi_0)} \\ S_i^z &= [\sqrt{S^2 - 2\rho_0 u^2} + \sqrt{S^2 - 2\rho_0 v^2} + (-1)^{i_x}(\sqrt{S^2 - 2\rho_0 u^2} - \sqrt{S^2 - 2\rho_0 v^2})]/2 \end{aligned} \quad (25)$$

where the sign  $\pm\sqrt{S^2 - |\mathbf{S}^+|^2}$  is chosen such that  $S_i^z$  reproduce the Z-FM when  $\rho_0 \rightarrow 0$ . It leads to the spin-orbital order in the IC-SkX phase when  $h_* < H < h_{c2}$  which is the fixed point in the IC-SkX phase where one of the two sublattices  $S_i^z = 0$ .

After identifying the even/odd  $i_x$  to be  $A/B$  sub-lattice, one can also calculate

$$\lim_{h \rightarrow h_{c2}^+} \frac{|S_A^+|}{|S_B^+|} = \lim_{h \rightarrow h_{c2}^+} \frac{v}{u} = \sqrt{\sin^4 2\beta + \sin^2 2\beta} - \sqrt{\sin^4 2\beta - \cos^2 2\beta} \quad (26)$$

which indeed matches the ratio  $|S_A^+|/|S_B^+|$  calculated using the SWE from below  $h_{c2}^-$  shown in Eq.C4.

It is important to stress that the quantum spin in Eq.15 ( or Eq.26 ) is linearly related to the magnon operator, in contrast to many other cases where the quantum spin is quadratically represented in terms of spinon operators. Amazingly, despite the Bogliubov transformation matrix element  $u$  and  $v$  are only well defined above  $h > h_{c2}$ . We can still take the two as two phenomenological parameters in Eq.15 ( or Eq.26 ) inside the IC-SkX below  $h < h_{c2}$ . It indeed matches the microscopic calculation using SWE in [14]. Note that Eq.26 takes the identical form as Eq.7 after replacing the Bogliubov transformation matrix elements  $u, v$  by the unitary transformation matrix elements  $c, s$ . It is remarkable that one can extend the unitary transformation matrix elements  $c, s$  in the Z-x phase above  $h_{c1}$  and the Bogliubov transformation matrix elements  $u, v$  in the FM state below  $h_{c2}$  and reach the same spin-orbital structure of the IC-SkX phase in Eq.7 and Eq.26 respectively.

## B. Excitation spectrum: exotic gapless Goldstone and gapped roton mode

When  $\mu < 0$ , it is in the Z-FM state with  $\langle \psi_\alpha \rangle = 0, \alpha = 1, 2$ , expanding the effective action upto the second order in  $\psi_\alpha$  leads to:

$$\mathcal{S}_2 = \int d\tau d^2r \sum_{\alpha=1,2} (\psi_\alpha^* \partial_\tau \psi_\alpha + v_x^2 |\partial_x \psi_\alpha|^2 + v_y^2 |\partial_y \psi_\alpha|^2 - \mu |\psi_\alpha|^2) \quad (27)$$

which lead to 2 degenerate gapped modes

$$\omega_{1,2} = -\mu + v_x^2 k_x^2 + v_y^2 k_y^2 \quad (28)$$

which matches the result achieved by SWE in [14].

When  $\mu > 0$ , it is in IC-SkX state with  $\langle \psi_\alpha \rangle = \sqrt{\rho_\alpha} e^{i\phi_\alpha}, \alpha = 1, 2$ , one may write the fluctuations in the polar coordinate as  $\psi_\alpha = \sqrt{\rho_0/2 + \delta\rho_\alpha} e^{i(\phi_0 + \delta\phi_\alpha)}$  and expand the action upto the second order in the fluctuations. It turns out to be convenient to introduce  $\delta\rho_\pm = (\delta\rho_1 \pm \delta\rho_2)/\sqrt{2}$  and  $\delta\phi_\pm = (\delta\phi_1 \pm \delta\phi_2)/\sqrt{2}$  where the action becomes

$$\begin{aligned} \mathcal{S}_2 &= \int d\tau d^2r \left( i\delta\rho_+ \partial_\tau \delta\phi_+ + \frac{1}{2\rho_0} [v_x^2 (\partial_x \delta\rho_+) + v_y^2 (\partial_y \delta\rho_+)] + \frac{\rho_0}{2} [v_x^2 (\partial_x \delta\phi_+) + v_y^2 (\partial_y \delta\phi_+)] + 2(U - A)(\delta\rho_+)^2 \right. \\ &\quad + i\delta\rho_- \partial_\tau \delta\phi_- + \frac{1}{2\rho_0} [v_x^2 (\partial_x \delta\rho_-) + v_y^2 (\partial_y \delta\rho_-)] + \frac{\rho_0}{2} [v_x^2 (\partial_x \delta\phi_-) + v_y^2 (\partial_y \delta\phi_-)] + 2A(\delta\rho_-)^2 + 2A\rho_0^2 (\delta\phi_-)^2 \\ &\quad \left. - V_1 \rho_0 [4\delta\rho_+ \partial_y \delta\phi_+ + 2\delta\rho_- \partial_y \delta\phi_-] - V_2 \rho_0 [4\delta\rho_+ \partial_y \delta\phi_+ - 2\delta\rho_- \partial_y \delta\phi_-] \right) \end{aligned} \quad (29)$$

which leads to one exotic gapless Goldstone and one exotic gapped roton mode

$$\begin{aligned} \omega_{+, \mathbf{k}} &= \sqrt{4\rho_0(U - A)(v_x^2 k_x^2 + v_y^2 k_y^2)} - (4V_1 + 2V_2)\rho_0 k_y, \\ \omega_{-, \mathbf{k}} &= \sqrt{16\rho_0^2 A^2 + 8\rho_0 A(v_x^2 k_x^2 + v_y^2 k_y^2)} - (4V_1 - 2V_2)\rho_0 k_y \end{aligned} \quad (30)$$



where the Goldstone mode achieved from below  $h_{c2}$  takes the same form as that in Eq.13 achieved from above  $h_{c1}$ . This match is a good check on the consistency between the effective action from  $h_{c2}$  down and that from  $h_{c1}$  up.

At the mirror symmetric point  $\beta = \pi/4$  ( $k_0 = \pi/2$ ) which dictates  $V_1 = V_2 = C_2 = 0$ . Eq.21 in the  $\psi_{1,2}$  representation becomes:

$$\begin{aligned} S_2 = \int d\tau d^2r & \left( i\delta\rho_+ \partial_\tau \delta\phi_+ + \frac{1}{2\rho_0} [v_x^2(\partial_x \delta\rho_+) + v_y^2(\partial_y \delta\rho_+)] + \frac{\rho_0}{2} [v_x^2(\partial_x \delta\phi_+) + v_y^2(\partial_y \delta\phi_+)] + 2(U - A)(\delta\rho_+)^2 \right. \\ & + i\delta\rho_- \partial_\tau \delta\phi_- + \frac{1}{2\rho_0} [v_x^2(\partial_x \delta\rho_-) + v_y^2(\partial_y \delta\rho_-)] + \frac{\rho_0}{2} [v_x^2(\partial_x \delta\phi_-) + v_y^2(\partial_y \delta\phi_-)] + 2A(\delta\rho_-)^2 + 2A\rho_0^2(\delta\phi_-)^2 \\ & \left. + 4B_2 \cos 4\phi_0 [(\delta\rho_-)^2 - \rho_0^2(\delta\phi_-)^2] - 8B_2 \sin 4\phi_0 (\delta\rho_-)(\delta\phi_-) \right) \end{aligned} \quad (31)$$

where one can see the  $B_2$  term are endowed with a  $\phi_0$  dependence and only affects the gapped roton  $-$  mode, but not the gapless Goldstone  $+$  mode. This is expected, because this  $B_2$  term breaks only the  $U(1)_{ic}$ , but not the  $U(1)_{soc}$  symmetry.

The excitations can be extracted as:

$$\begin{aligned} \omega_{+,k} &= \sqrt{4\rho_0(U - A)(v_x^2 k_x^2 + v_y^2 k_y^2)}, \\ \omega_{-,k} &= \sqrt{16\rho_0^2(A^2 - 4B_2^2) + 8\rho_0 A(v_x^2 k_x^2 + v_y^2 k_y^2)} \end{aligned} \quad (32)$$

which recover to the conventional form and are independent of  $\phi_0$  as expected. It also indicate the Umklapp term at  $\beta = \pi/4$  does not affect the Goldstone mode, but decrease the roton gap.

### C. QPT: Two Type-II dangerously irrelevant operators away from the mirror symmetric point

When away from the mirror symmetric point, the Umklapp terms drop out, but the  $V_1, V_2$  term move in. The symmetry is enlarged to  $U(1)_{soc} \times U(1)_{ic}$  which is spontaneously broken down to  $[U(1)_{soc} \times U(1)_{ic}]_D$  in the IC-SkX phase leading to one Goldstone mode. In fact, there is also a  $Z_2$  exchange symmetry between  $\psi_1$  and  $\psi_2$  ( or  $\psi_+$  and  $\psi_-$  ) which is also broken inside the IC-SkX phase. The universality class can be best seen in the  $\psi_\pm$  basis Eq.18. Because it is the Ising limit, so the saddle point solution  $\langle\psi_- \rangle = 0$  or  $\langle\psi_+ \rangle = 0$  still respects  $[U(1)_{soc} \times U(1)_{ic}]_D$  generated by  $\mathcal{T}_y^n \times \mathcal{R}(nk_y^0)$ . The two different solutions correspond to the exchange of A and B sublattices in the IC-SkX phase. As shown above, the Two Type-II dangerously irrelevant operators  $V_1, V_2$  modify both the Goldstone and the roton mode to the exotic form.

In one appendix of [21], we studied the SF-Mott transition in a one component boson at integer filling subject to a  $\pi$  flux and reached the same effective action as Eq.18 upto to the quartic order, also in Ising limit. However, there are no dangerously irrelevant operators. In [40], we studied the SF to charge density wave (CDW) transition one component boson at half filling in a honeycomb lattice with nearest neighbor repulsive interaction. We also reached a similar effective action as Eq.18, also in the Ising limit, with  $\psi_\pm$  standing for the vortex degree of freedoms hopping in a dual triangular lattice which couple to a gapless fluctuating  $U(1)$  gauge field. The saddle point solution  $\langle\psi_- \rangle = 0, \langle\psi_+ \rangle \neq 0$  or  $\langle\psi_- \rangle \neq 0, \langle\psi_+ \rangle = 0$  correspond to the two CDW states which breaks the  $U(1)$  gauge symmetry, open a gap through the Higgs mechanism. There are no dangerously irrelevant operators either.

At the mirror symmetric point  $\beta = \pi/4$ , the  $V_1, V_2$  term drop out, but the Umklapp term Eq.20 move in Eq.21. It remains in the Ising limit where one of  $\psi_\pm$  vanishes. So the Umklapp term will not change the universality class. Due to the absence of the two Type-II dangerously irrelevant operators, the Goldstone and roton modes recover to the conventional ones.

## IV. QUANTUM PHASE TRANSITION AT $h_{c2}$ AND IN THE LEFT RANGE $0 < \beta < \beta_1$ : ORDER PARAMETER REDUCTION

The SWE in the FM state above  $h_{c2}$  leads to Eq.B12. It is the  $\alpha_{\mathbf{k}}$  magnon condensation which leads to the QPT from the FM state to the canted phase at  $h_{c2}$  in the left range  $0 < \beta < \beta_1$ . In contrast to the middle range presented in the previous section, the condensation happens at the two commensurate momentum 0 and  $\mathbf{Q} = \mathbf{K}_2 - \mathbf{K}_1 = (\pi, 0)$ , so the order parameter takes the form:

$$\langle\alpha_{\mathbf{k}}\rangle = \psi_1 \delta_{\mathbf{k},0} + \psi_2 \delta_{\mathbf{k},\mathbf{Q}} \quad (33)$$

where  $\psi_1, \psi_2$  are the two complex order parameters.

One must use the Bogoliubov transformation Eq.(B10) to establish the connection between the quantum spin and the two complex order parameters:

$$\langle S_i^+ \rangle \propto u[\psi_1 + (-1)^{i_x} \psi_2] + v[\psi_1^* - (-1)^{i_x} \psi_2^*] \propto (\psi_1 + \psi_1^*) + (-1)^{i_x} (\psi_2 - \psi_2^*) = \psi_R + (-1)^{i_x} i\psi_I \quad (34)$$

where we have used the fact  $u = u_0 = u_{\mathbf{Q}} = \infty$  and  $v = v_0 = -v_{\mathbf{Q}} = \infty$ , but their ratio  $u/v = 1$ , so they can be factored out. In fact, the Bogoliubov transformation matrix elements  $u, v$  are only finite at IC-momentum, but diverge at C-momentum.

Naively, similar to the last section, one may still need to use the two complex order parameters  $\psi_1, \psi_2$  to construct the effective action. However, Eq.34 shows that the relevant order parameter maybe just ONE complex field as  $\psi = \psi_1 + \psi_1^* + \psi_2 - \psi_2^*$  whose real part  $\psi_R = \Re\psi = \psi_1 + \psi_1^*$  and imaginary part  $\psi_I = \Im\psi = -i(\psi_2 - \psi_2^*)$  can be used to determine the quantum spin uniquely. This observation is further substantiated by the crucial fact that under  $U(1)_{\text{soc}}$ ,  $\psi \rightarrow e^{i\phi_0} \psi$  as shown in the item 4 below. One may call this new phenomenon as order parameter reduction from 2 to 1 which simplifies the following analysis considerably. Intuitively, one may also think  $\psi$  as a composite operator consisting of two components  $\psi_1, \psi_2$ , one leads to its real part, the other leads to its imaginary part. The two components will emerge as two independent ones when getting into a IC-phase. This fractionization process indeed happens as shown in Sec V.

Because the Z-FM state breaks no symmetry of the Hamiltonian, so one can study how the single order parameter  $\psi$  transform under symmetries of  $\mathcal{H}$ ,

1. Translation:  $\mathcal{T}_x : \psi(x, y) \rightarrow \psi^*(x, y)$  and  $\mathcal{T}_y : \psi(x, y) \rightarrow \psi(x, y)$ ;
2. Space reflection:  $\mathcal{I}_y : \psi(x, y) \rightarrow \psi(-x, y)$ ;
3. Spin reflection:  $\mathcal{P}_z : \psi(x, y) \rightarrow -\psi(x, y)$ ;
4. Spin-orbital U(1) rotation:  $\mathcal{R} : \psi(x, y) \rightarrow e^{i\phi_0} \psi(x, y)$ ;
5. Spin-orbital reflection:  $\mathcal{T} \circ \mathcal{I}_x \circ \mathcal{P}_x : \psi(x, y) \rightarrow -\psi^*(x, -y)$  and  $\mathcal{T} \circ \mathcal{I}_x \circ \mathcal{P}_y : \psi(x, y) \rightarrow \psi^*(x, -y)$ ;
6. Enlarged mirror symmetry at  $\beta = \pi/4$ :  $\mathcal{T} \circ \mathcal{M} : \psi(x, y) \rightarrow -\psi^*(x, y)$ . ( of course,  $\beta = \pi/4$  is beyond this regime )

The above symmetry analysis leads to the following one complex component effective action with the dynamic exponent  $z = 1$  In the continuum limit:

$$\mathcal{S} = \int d\tau d^2r [(\partial_\tau \psi^* - ic\partial_y \psi^*)(\partial_\tau \psi - ic\partial_y \psi) + v_x^2 |\partial_x \psi|^2 + v_y^2 |\partial_y \psi|^2 - \mu |\psi|^2 + U |\psi|^4] \quad (35)$$

where one need to realize  $(\partial_\tau \psi^* - ic\partial_y \psi^*)(\partial_\tau \psi - ic\partial_y \psi) \neq |(\partial_\tau \psi - ic\partial_y \psi)|^2$ .

Our microscopic calculation shows that  $\mu = h_{c2} - h, U > 0$  and  $c \propto \sin 2\beta$ . Due to the magnon condensations at only the two C-momenta, the odd derivative in  $\partial_y$  terms only appear in the combination with  $\partial_\tau - ic\partial_y$  which specifies the kinetic term in Eq.35.

Note that  $c = 0$  vanishes at the Abelian point  $\beta = 0$ . This is because there is an enlarged space reflection  $\mathcal{I}_x : \psi(x, y) \rightarrow \psi(x, -y)$  because at the Abelian point  $\beta = 0$ . See also appendix E.

### A. The spin-orbital order of the ground state

At the mean-field level, we can substitute  $\psi \rightarrow \sqrt{\rho_0} e^{i\phi_0}$  into the effective action Eq.35

$$\mathcal{S} = -\mu\rho_0 + U\rho_0^2 \quad (36)$$

When  $\mu = h_{c2} - h < 0$ , it is in the Z-FM state with  $\langle \psi \rangle = 0$ . When  $\mu > 0$ , it is in the canted phase with  $\langle \psi \rangle = \sqrt{\rho_0} e^{i\phi_0}$  where  $\rho_0 = \mu/2U$  and  $\phi_0$  is a arbitrary angle due to the  $U(1)_{\text{soc}}$  symmetry.

Combing Eq.34 with the constraint  $|\mathbf{S}_i|^2 = S^2$ , one obtain the spin-orbital order of the canted phase as:

$$\langle S_i^+ \rangle = \sqrt{\rho_0} [\cos \phi_0 + (-1)^{i_x} i \sin \phi_0], \quad \langle S_i^z \rangle = \sqrt{S^2 - \rho_0} \quad (37)$$

where the sign of  $\pm \sqrt{S^2 - |\mathbf{S}^+|^2}$  is chosen such that  $S_i^z$  reproduces the Z-FM order when  $\rho_0 \rightarrow 0$ . It is obvious Eq.(37) indeed matches the spin-orbital order of the canted phase achieved by the microscopic SWE calculations in [14]. Remarkably, despite we only use one complex order parameter  $\psi$ , one can still use its real and imaginary part to stand for the transverse quantum spin with TWO C- ordering wavevectors  $(0, 0)$  and  $\mathbf{Q} = \mathbf{K}_2 - \mathbf{K}_1 = (\pi, 0)$ .

### B. Excitation spectrum: Exotic Goldstone mode and Higgs mode

In the Z-FM phase,  $\mu < 0$ , one can write  $\psi = \psi_R + i\psi_I$  as its real part and imaginary part and expand the action upto second order

$$\mathcal{S} = \int d\tau d^2r \sum_{\alpha=R,I} [(\partial_\tau \psi_\alpha - ic\partial_y \psi_\alpha)^2 + v_x^2 (\partial_x \psi_\alpha)^2 + v_y^2 (\partial_y \psi_\alpha)^2 - \mu(\psi_\alpha)^2] \quad (38)$$

which lead to 2 degenerate gapped modes

$$\omega_{R,I} = \sqrt{-\mu + v_x^2 k_x^2 + v_y^2 k_y^2} - ck_y \quad (39)$$

which match the results achieved by SWE in [14]. Eq.39 can be contrasted to Eq.28, both are gapped modes in the Z-x phase. The difference is that the latter is expanded around the two true in-commensurate minima  $\mathbf{K}_1 = (0, k_0)$ ,  $\mathbf{K}_2 = (\pi, k_0)$  whose constant contour is shown in Fig.1b and indicates the dynamic exponent  $z = 2$  while the former is expanded around the two commensurate momentum  $(0, 0)$  and  $(\pi, 0)$  which are not the true minima as shown in Fig.1b, it indicates the dynamic exponent  $z = 1$ .

In the canted phase,  $\mu > 0$ , we can write the fluctuations in the polar coordinates  $\psi = \sqrt{\rho_0 + \delta\rho} e^{i(\phi_0 + \delta\phi)}$  and expand the action up to the second order in the fluctuations:

$$\begin{aligned} \mathcal{S} = \frac{1}{2\rho_0} \int d\tau d^2r & \left( [(\partial_\tau - ic\partial_y)\delta\rho]^2 + [v_x^2 (\partial_x \delta\rho)^2 + v_y^2 (\partial_y \delta\rho)^2] + 4\rho_0 U(\delta\rho)^2 \right. \\ & \left. + \rho_0^2 [(\partial_\tau + ic\partial_y)\delta\phi]^2 + \rho_0^2 [v_x^2 (\partial_x \delta\phi)^2 + v_y^2 (\partial_y \delta\phi)^2] \right) \end{aligned} \quad (40)$$

which due to  $z = 1$ , leads to one gapless Goldstone mode and one gapped Higgs mode [47]

$$\begin{aligned} \omega_H &= \sqrt{4\rho_0 U + v_x^2 k_x^2 + v_y^2 k_y^2} - ck_y \\ \omega_G &= \sqrt{v_x^2 k_x^2 + v_y^2 k_y^2} - ck_y \end{aligned} \quad (41)$$

where the Goldstone mode reproduce the superfluid mode and the Higgs mode reproduce the "roton" mode achieved by SWE in [14].

Note that it is the  $z = 1$  which ensures the separation of the real part from the imaginary part when  $\mu < 0$  in the Z-x phase in Eq.39 and the separation of the Higgs mode from the Goldstone mode when  $\mu > 0$  in the canted phase in Eq.42. Intuitively, one can say the two degenerate gapped modes in Eq.39 turn into the Goldstone mode and the Higgs mode in Eq.42 through the QPT from the Z-x phase to the canted phase at  $h_{c2}$ .

### C. The QCP: a boosted SF-Mott transition

The effective action Eq.35 can be transformed into a 2d SF-Mott transition in a boosted frame along  $y$ - axis by performing a Galileo transformation  $y' = y - ct, t' = t$ . In the imaginary time  $\tau = it$ , it implies  $\partial'_y \rightarrow \partial_y, \partial'_\tau \rightarrow \partial_\tau - ic\partial_y$ . So the effective action becomes the same as as the 2d SF-Mott transition in a boosted frame. It is exactly marginal at  $h_{c2}$  suggesting a line of fixed points. However, it is the boost which drives the quantum Lifshitz transition from the canted phase to the IC-SkX phase at  $\beta = \beta_L$  as to be discussed in Sec.V. The mechanism for how a SOC generates such a boost is not known and need to be investigated further. If the dynamic exponent  $z = 1$  receives anomalous dimension need to be examined also [53].

At the Abelian point  $\beta = 0, c = 0$ , the boost disappears, so the transition at  $h_{c2}$  is nothing but the 3d XY universality class. In fact, as shown in [13–15], the Hamiltonian at this Abelian point can be mapped to a FM Heisenberg model in a staggered Zeeman field along  $x$ - direction. As shown in the appendix F, it is dramatically different than the AFM in a uniform field which has the dynamic exponent  $z = 2$ .

### D. Contrast to a putative supersolid

In the previous works on putative supersolids in a continuum system driven by the roton collapse [42–45], There is a crucial coupling term which couples the lattice phonon modes to the SF mode.  $ia_{\alpha\beta}u_{\alpha\beta}\partial_\tau\theta$  where  $u_{\alpha\beta} = \frac{1}{2}(\partial_\alpha u_\beta + \partial_\beta u_\alpha)$  is the linearized strain tensor. The factor of  $i$  is important in this coupling. By integration by parts,

this term can also be written as  $a_{\alpha\beta}(\partial_\tau u_\beta \partial_\alpha \theta + \partial_\tau u_\alpha \partial_\beta \theta)$  which has the clear physical meaning of the coupling between the SF velocity  $\partial_\alpha \theta$  and the velocity of the lattice vibration  $\partial_\tau u_\beta$ . It is this coupling between the phonon mode and the superfluid mode which leads to the two gapless low energy modes inside the SS. They have their own characteristics which could be detected by experiments. The two gapless modes result from  $U(1)_c \times U(1)_l \rightarrow 1$  symmetry breaking, the first is the phase, the second the lattice translational symmetry breaking. In a contrast, the coset Eq.22 only leads to one gapless mode and one roton mode. So the second term  $-i2c\partial_\tau \psi^* \partial_y \psi$  in Eq.50 is very similar to such a coupling in the putative supersolid.

## V. QUANTUM LIFSHITZ TRANSITION AT THE LEFT CRITICAL FIELD $\beta_L$

Inside the canted phase at a fixed  $h$ , as the SOC parameter increases, there is a quantum Lifshitz transition from the canted phase to the IC-SkX driven by the instability of the Goldstone mode in Eq.41 ( Fig.1 ). Because the gapped Higgs mode remains un-critical across the transition, one can simply drop it. Although the Goldstone mode to the quadratic order in Eq.41 is enough inside the canted phase. When studying the transition to the IC-SkX, one must incorporate higher derivative terms and also higher order terms. A simple symmetry analysis leads to the following bosonic quantum Lifshitz transition at the left critical SOC parameter  $\beta_L$  (Fig.1) which extends Eq.41 to include higher derivative terms and also higher order terms:

$$\mathcal{S}_L = \int d\tau d^2r [(\partial_\tau \phi - ic\partial_y \phi)^2 + v_x^2(\partial_x \phi)^2 + v_y^2(\partial_y \phi)^2 + a(\partial_y^2 \phi)^2 + b(\partial_y \phi)^4] \quad (42)$$

where  $a, b > 0$  and  $c \propto \sin(2\beta)$ , especially  $v_y^2 - c^2 = \beta - \beta_L$  is the tuning parameter. At a fixed  $h$ , as  $\beta$  increases, the boost  $c$  also increases. When  $c$  reaches the value of  $v_y$ , it signifies an instability of the Goldstone mode which drives the quantum Lifshitz transition from the canted phase to the IC-SkX phase. [27]. A simple scaling shows that when  $z = 1$  inside the canted phase  $[a] = -2, [b] = -3$ , so they are irrelevant inside the IC-SkX phase, but become important near the transition as to be shown in the following.

### A. Obtain the spin-orbital order of the IC-SkX from the canted phase: Order parameter fractionization

The mean-field state can be written as  $\phi = \phi_0 + k_0 y$ . Substituting it to the effective action Eq.42, we obtain

$$\mathcal{S}_0 \propto (v_y^2 - c^2)k_0^2 + bk_0^4 \quad (43)$$

At a lower boost  $c^2 < v_y^2$ ,  $k_0 = 0$  is in the C- Canted phase.

At a high boost  $c^2 > v_y^2$ ,  $k_0^2 = (c^2 - v_y^2)/2b$  is inside the IC-SkX phase with the modulation  $k_0$  along the  $y$ - axis. The sign of  $k_0$  is determined by the sign of  $c$ , i.e.  $k_0 = \text{sgn}(c)\sqrt{k_0^2}$ . Substituting  $\phi = \phi_0 + k_0 y$  back to the phase of the complex order parameter leads to  $\psi = \psi_1 + \psi_1^* + \psi_2 - \psi_2^* \propto e^{i(\phi_0 + k_0 y)}$ , which admits a physical solution with  $\psi_\alpha = \tilde{\psi}_\alpha e^{ik_0 y}$ ,  $\alpha = 1, 2$ . Thus Eq.34 in the canted phase turns into:

$$\langle S_i^+ \rangle = u[\tilde{\psi}_1 + (-1)^{i_x} \tilde{\psi}_2] e^{ik_0 i_y} + v[\tilde{\psi}_1^* - (-1)^{i_x} \tilde{\psi}_2^*] e^{-ik_0 i_y} \quad (44)$$

where we put back the two phenomenological parameters  $u$  and  $v$ . This is because  $u/v \neq 1$  any more due to a nonzero  $k_0$ . Thus it reproduces the IC-SkX phase in Eq.15 when  $c^2 > v_y^2$ . This is equivalent to shift the two condensation wave-vectors in Eq.33 to  $\langle \mathbf{a}_\mathbf{k} \rangle = \tilde{\psi}_1 \delta_{\mathbf{k}, 0+(0, k_0)} + \tilde{\psi}_2 \delta_{\mathbf{k}, \mathbf{Q}+(0, k_0)}$  at the very beginning.

So in the quantum Lifshitz transition, there is a C-IC transition from the canted phase to the IC-SkX phase, the order parameter fractionize from One complex order parameter  $\psi = \psi_1 + \psi_1^* + \psi_2 - \psi_2^*$  into TWO independent ones  $\psi_1, \psi_2$ . One may also look at the quantum Lifshitz transition from the dual point of view: there is a IC-C transition from the IC-SkX phase to the canted phase, the TWO complex order parameters  $\psi_1, \psi_2$  confine into just One complex order parameter  $\psi = \psi_1 + \psi_1^* + \psi_2 - \psi_2^*$ . The dynamic exponent changes from  $z = 1$  to  $z = 2$ , the Higgs mode in Eq.42 in the canted phase automatically changes to the roton mode in Eq.31 inside the IC-SKX phase. In fact, the the order parameter fractionization already shows its sign even above the  $h_{c2}$  inside the Z-FM phase: Eq.39 containing 2 degenerate gapped modes with real and imaginary part above canted phase evolve into Eq.28 containing the 2 degenerate gapped modes with two complex order parameters above the IC-SkX phase.

### B. The excitation spectrum in the canted phase and IC-SkX phase

At a low boost  $c^2 < v_y^2$ , the quantum phase fluctuation can be written as  $\phi = \phi_0 + \delta\phi$ . Expanding the action upto second order leads to:

$$\mathcal{S}_{2c} = \int d\tau d^2r [(\partial_\tau \phi - ic\partial_y \phi)^2 + v_x^2(\partial_x \phi)^2 + v_y^2(\partial_y \phi)^2] \quad (45)$$

which reproduces the gapless Goldstone mode in Eq.42 inside the canted phase:

$$\omega_{\mathbf{k}} = \sqrt{v_x^2 k_x^2 + v_y^2 k_y^2} - ck_y \quad (46)$$

At a high boost  $c^2 > v_y^2$ , the quantum phase fluctuations can be written as  $\phi = \phi_0 + k_0 y + \delta\phi$ . Expanding the action upto the second order in the phase fluctuations leads to

$$\mathcal{S}_{2ic} = \int d\tau d^2r [(\partial_\tau \phi - ic\partial_y \phi)^2 + v_x^2(\partial_x \phi)^2 + (v_y^2 + 6bk_0^2)(\partial_y \phi)^2] \quad (47)$$

which reproduces the gapless Goldstone mode in Eq.31 or Eq.13 inside the IC-SkX phase:

$$\begin{aligned} \omega_{\mathbf{k}} &= \sqrt{v_x^2 k_x^2 + (v_y^2 + 6bk_0^2)k_y^2 + ak_y^4} - ck_y \\ &= \sqrt{v_x^2 k_x^2 + (3c^2 - 2v_y^2)k_y^2 + ak_y^4} - ck_y \end{aligned} \quad (48)$$

where one can see  $3c^2 - 2v_y^2 > 2(c^2 - v_y^2) + c^2 > c^2$  when  $c^2 > v_y^2$ , thus the  $\omega_{\mathbf{k}}$  is stable in IC-SkX phase.

### C. The exotic QCP scaling with the dynamic exponents ( $z_x = 3/2, z_y = 3$ )

It is instructive to expand the first kinetic term in Eq.42 as:

$$\mathcal{S} = \int d\tau d^2r [Z(\partial_\tau \phi)^2 - 2iv_y \partial_\tau \phi \partial_y \phi + v_x^2(\partial_x \phi)^2 + \gamma(\partial_y \phi)^2 + a(\partial_y^2 \phi)^2 + b(\partial_y \phi)^4] \quad (49)$$

where  $Z$  is introduced to keep track of the renormalization of  $(\partial_\tau \phi)^2$  and  $\gamma = v_y^2 - c^2 = \beta - \beta_L$  is the tuning parameter.

The scaling  $\omega \sim k_y^3, k_x \sim k_y^2$  leads to the exotic the dynamic exponents ( $z_x = 3/2, z_y = 3$ ). Then one can get the scaling dimension of  $[\gamma] = 2$  which is relevant, as expected, to tune the transition. One can also find that  $[Z] = [b] = -2 < 0$ , so both are leading irrelevant operators[27]. Setting  $Z = b = 0$  in Eq.49 leads to the fixed action at the QCP where  $\gamma = 0$ . Possible connections with Rokhsar-Kivelson's Quantum Dimer (QD) model in a square lattice in its height representation [29–31] to describe the transitions between VBS and associated deconfined QCP need to be explored further. Of course, our system is a quantum spin one.

### D. Multi-critical point M

Expanding the kinetic term in Eq.35 leads to

$$\mathcal{S} = \int d\tau d^2r [Z|\partial_\tau \psi|^2 - i2c\partial_\tau \psi^* \partial_y \psi + v_x^2|\partial_x \psi|^2 + a|\partial_y^2 \psi|^2 + \gamma|\partial_y \psi|^2 - \mu|\psi|^2 + U|\psi|^4] \quad (50)$$

where  $\mu = h_{c2} - h$  and  $\gamma = v_y^2 - c^2$ . Moving along  $h_{c2}$  in the left range  $0 < \beta < \beta_1$ ,  $\gamma$  decreases until reaching the Multi-critical (M) point  $\gamma = 0$ . So there are two relevant operators  $\mu$  and  $\gamma$ , with the scaling dimensions  $[\gamma] = 2, [\mu] = 4$  respectively. Then there is a order parameter fractionization at the  $M$  point: one complex order parameter  $\psi$  splits into  $\psi_1, \psi_2$ , C to IC transition, dynamic exponent changes from  $z = 1$  to  $z = 2$  through the M point with ( $z_x = 3/2, z_y = 3$ ).

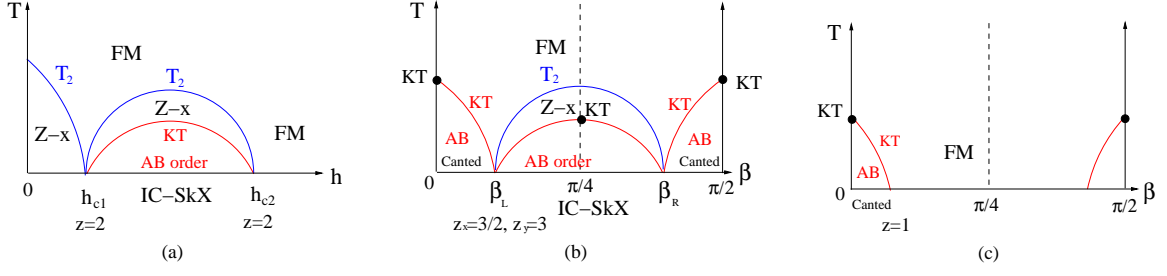


FIG. 2. (Color online) Finite temperature phase transitions above the three quantum C-IC transition at  $T = 0$ . The zero temperature QPT with various dynamic exponents are also indicated. (a) At a fixed  $\beta$ . At  $T = 0$ , there is a quantum C-IC transition from the Z-x to the IC-SkX at  $h = h_{c1}$  and from the IC-SkX to the FM at  $h = h_{c2}$  shown in Fig.1. There is a finite temperature Ising transition  $T_2$  above the Z-x state. The IC-SkX has only an algebraic (denoted as AB in the figure) order in the transverse spin components before getting to the Z-x state at  $T = T_{KT}$ , then melt into the FM state at  $T_2$ . As shown in the text, the transition at  $T_{KT}$  is the same universality class as the Kosterlitz-Thouless (KT) transition, even away from the mirror symmetric point  $\beta = \pi/4$  where  $T_{KT}$  reaches the maximum value. as shown as the black dot in (b). (b) At a fixed  $h$ . At  $T = 0$ , there is a quantum C-IC transition from the canted phase to the IC-SkX at  $\beta_L$  and from the IC-SkX to the mirror reflected canted phase at  $\beta_R = \pi/2 - \beta_L$  shown in Fig.1. There is a finite temperature KT transition above the canted state, even away from the two Abelian points  $\beta = 0, \pi/2$  where  $T_{KT}$  reaches the maximum. There is a mirror symmetry about  $\beta = \pi/4$  where the IC-SkX reduces to the  $2 \times 4$  SkX and the  $T_{KT}$  reaches the maximum. Replacing the IC-SkX in (b) by the FM leads to (c) where there is a C-C transition from the canted to the FM state at  $T = 0$  in Fig.1. As argued in [14], all the critical temperatures  $T_c \sim \Delta \sim 2SJ = NJ \sim N \times 0.2nK$  where the  $N$  is the number of atoms per site, so all the critical temperatures can be easily increased above the experimentally reachable temperatures simply by increasing the number of spinor atoms on every lattice site. Fig.2a can be contrasted to the experimental temperature versus Zeeman field phase diagrams in [54, 55].

## VI. FINITE TEMPERATURE PHASE TRANSITIONS

Any experiments are performed at finite temperatures which are controlled by the quantum phases and phase transitions at  $T = 0$  in Fig.1 and Fig.2. The experiments in [54, 55] examined carefully the interplay of the temperature against the Zeeman field. Here, we discuss the effects of finite temperatures. The thermodynamic quantities at a small finite  $T$  was discussed in [14]. Here, we focus on the spin-spin correlation functions at a finite  $T$ .

As argued in [13], there is only one finite temperature phase transition in the Ising universality class [15] above the  $Z-x$  phase. The FM state breaks no symmetries of the Hamiltonian, so no transitions above it. So we only need to discuss the finite temperature transitions above the canted phase and IC-SkX state as shown in Fig.2a.

At a finite temperature, setting the quantum fluctuations (the  $\partial_\tau$  term) vanishing, in Eq.45 or Eq.47, then both equations reduce to

$$\mathcal{S}_{KT} = \int d\tau d^2r [v_x^2 (\partial_x \phi)^2 + \gamma (\partial_y \phi)^2] \quad (51)$$

where  $\gamma = v_y^2 - c^2$  inside the canted phase and  $\gamma = 2(c^2 - v_y^2)$  inside the IC-SkX phase. It indicates the finite temperature phase transition is still in Kosterlitz-Thouless (KT) universality class, despite the exotic form of the spectrum of the Goldstone mode.

1. *The canted phases:* In the canted phase, from 45, one can see that at any  $T > 0$ , the Goldstone mode fluctuations Eq.42 lead to  $\langle S^+ \rangle = 0$  in Eq.37, so the transverse spin correlation functions display algebraic orders at the two ordering wavevectors  $\vec{Q}_1 = (0, 0)$  and  $\vec{Q}_2 = (\pi, 0)$ . So there is only one finite temperature phase transition  $T_{KT}$  driven by the topological defects in the phase  $\phi$  in Eq.51 above the canted phase to destroy the algebraic order (Fig.2b,c).

The transverse Bragg spectroscopy in the canted phase at  $T = 0$  will display sharp peaks at  $\vec{Q}_1 = (0, 0)$  and  $\vec{Q}_2 = (\pi, 0)$ . However at  $0 < T < T_{KT}$ , the transverse peaks at  $\vec{Q}_1$  and  $\vec{Q}_2$  will be replaced by some power law singularities [48]. At  $T > T_{KT}$ , the power law singularities disappear.

2. *The IC-SkX phase:*

In the IC-SkX phase, from 45, one can see that at any  $T > 0$ , the Goldstone mode fluctuations Eqn.13 (or Eqn.31) also lead to  $\langle S^+ \rangle = 0$  in Eq.26 (or Eq.7), so the transverse spin correlation functions also display algebraic orders at the four in-commensurate ordering wavevectors  $(0, \pm k_y^0)$  and  $(\pi, \pm k_y^0)$ . So there are two finite temperature phase transitions above the IC-SkX state: one transition  $T_{KT}$  in the transverse spin sector to destroy the algebraic order, then another Ising  $Z_2$  transition in the longitudinal spin sector  $T_2$  to destroy the A and B sublattice  $Z_2$  symmetry

breaking as shown in Fig.1a. We also expect  $T_{KT} < T_2$ . Of course, at all the quantum phase transition boundaries in Fig.1,  $T_{KT} = T_2 = 0$ .

The elastic longitudinal Bragg spectroscopy in the IC-SkX at  $T = 0$  will display a sharp peak at  $(\pi, 0)$ , while the transverse Bragg spectroscopy will display sharp peaks at the four in-commensurate ordering wavevectors  $(0, \pm k_y^0)$  and  $(\pi, \pm k_y^0)$ . However at  $0 < T < T_{KT}$ , the transverse peaks at  $(0, \pm k_y^0)$  and  $(\pi, \pm k_y^0)$  will be replaced by some power law singularities [48], the longitudinal peak remains sharp. At  $T_{KT} < T < T_2$ , the power law singularities disappear, but the longitudinal peak remains sharp. When  $T > T_2$ , the longitudinal peak disappears.

Following the procedures [16, 38], one can also derive the scaling functions of spin-spin correlation functions at finite temperatures across the three C-IC quantum transitions in Fig.2a,b and also the C-C transition from the canted phase to the FM at the left or right segment of  $h_{c2}$  in Fig.2c.

## VII. IMPLICATIONS TO MATERIALS WITH STRONG SOC IN A ZEEMAN FIELD

Although the RFHM was derived as the strong coupling model of interacting spinor boson Hubbard model at integer fillings in the presence of SOC, we may just treat it as an effective lattice quantum spin model which incorporate competitions among AFM Heisenberg term, FM Kitaev term and Dzyaloshinskii-Moriya (DM) term. The Zeeman field adds a new dimension to these competitions. So RFHM + H can be used to not only to describe cold atom systems as described in details in [14], but also the universal features of some strongly correlated materials which host some of these interactions.

The IC-SkX phase in Fig.1 can be realized in some materials with a strong Dzyaloshinskii-Moriya (DM) interaction. Indeed, a 2D skyrmion lattice has been observed between  $h_{c1} = 50$  mT and  $h_{c2} = 70$  mT in some chiral magnets [39] MnSi or a thin film of  $\text{Fe}_{0.5}\text{Co}_{0.5}\text{Si}$  [39]. The effective actions Eq.5 and 18 or 21 may be used to describe the transitions near  $h_{c1}$  and  $h_{c2}$ .

Recently, there are flurries of theoretical and experimental researches to investigate the response of so called Kitaev materials to a Zeeman field. For example, in the 4d Kitaev material  $\alpha - \text{RuCl}_3$ , the ground state was shown experimentally to have a Zig-Zag order. In the application of a parallel magnetic field to the Zig-Zag magnetization [59], the system stays in the Zig-Zag order upto a lower critical field  $\mu_0 h_{c1} \sim 7$  T, becomes fully polarized above a upper critical field  $\mu_0 h_{c2} \sim 9$  T. Most interestingly, in the intermediate field range  $h_{c1} < \mu_0 H_l^* < h_{c2}$ , there is a possible field-induced quantum spin liquid (QSL) ground state displaying half-integer quantized thermal Hall conductivity plateau [54]. It hints a topologically protected chiral Majorana fermion edge mode. This edge mode is a direct consequence of the bulk Ising non-Abelian anyons in the Kitaev honeycomb lattice model subject to a small Zeeman field along [111] direction. The thermal Hall conductivity measurements in [55] between the ordering temperature of the Zig-Zag phase at  $T_N \sim 7$  K and the characteristic temperature of the Kitaev interaction  $J_K/k_B \sim 80$  K also shows signatures compatible with the itinerant Majorana fermions. This exciting, although still controversial discovery inspires further experimental and theoretical investigations. For example, by performing un-controlled parton construction mean field theory, the authors in [56] suggested that when the Kitaev model subjects to a Zeeman field along [111] direction, there could be a intermediate gapless  $U(1)$  QSL phase at an  $h_{c1} < h < h_{c2}$  with spinon Fermi surface which shows un-quantized thermal Hall conductivity. They also argued that the topological transitions at  $h_{c1}$  and  $h_{c2}$  are similar to the transition from a weak BCS pairing  $p_x + ip_y$  superconductor to a metal, then to a band insulator respectively. They also alerted to the readers that the gauge field fluctuations may be ignored in the gapped non-Abelian phase, but may be important in the gapless  $U(1)$  QSL phase, but very difficult to handle in a controlled way. Unfortunately, despite many appealing theoretical proposals summarized in [56], there is not a consistent and coherent theoretical framework which puts the Zig-Zag phase, the bulk gapped Kitaev non-abelian spin liquid phase with the half-integer quantized thermal Hall conductivity and the gapless putative spinon Fermi surface with an un-quantized thermal Hall conductivity in the same temperature versus the parallel Zeeman field phase diagram. Obviously, despite the Zig-Zag phase is a magnetic ordered ( therefore boring ) phase, it is the parent state, takes a large portion of the phase diagram, can not be ignored in giving a consistent description of experimental data in  $\alpha - \text{RuCl}_3$ .

Here, instead of directly working on Kitaev honeycomb lattice model, we take an alternative approach to study the interplay of the Zeeman field and SOC in a different strongly correlated quantum spin model called Rotated Heisenberg model along its solvable line with the  $U(1)_{\text{soc}}$  symmetry [13–15]. The global phase diagram Fig.1 achieved by both controlled microscopic SWE and symmetry based phenomenological effective actions is on a square lattice, so not directly relevant to the current experiments [54] yet. However, it does gives some physics universal to the competitions among AFM Heisenberg interaction, FM Kitaev interaction, DM term and the Zeeman term. For example, it indicates the interplay does lead to a highly non-trivial intermediate phase sandwiched between the magnetic ordered phase below the low critical field  $h < h_{c1}$  and the fully polarized FM phase above the upper critical field  $h > h_{c2}$ . Here, the intermediate phase is the canted phase at a small SOC and the IC-SkX phase at a large SOC. Both are gapless, so may show non-trivial ( although un-quantized ) thermal and thermal Hall conductivities. The Z-x phase in a square

lattice at a low field maybe used to mimic the Zig-Zag phase at a low field in a honeycomb lattice. Of course, the Z-FM phase at a high field always exists in any case. Both are gapped phases, so show exponentially suppressed thermal and thermal Hall conductivities. The IC-SkX phase could be easily melt into a QSL under some further quantum fluctuations. An extra SOC parameter in a honeycomb lattice may provide such quantum fluctuations. A future study on a honeycomb lattice with either spinor bosons or fermions [58] could be directly relevant. If the IC-SkX indeed melts into a QSL, then the transitions at  $h_{c1}$  and  $h_{c2}$  will become two Topological transitions driven by the condensation of spinons or  $Z_2$  flux or some fermions instead of some order parameter condensations.

## VIII. CONCLUSIONS AND DISCUSSIONS

From symmetry analysis, plus some inputs from the microscopic SWE calculations achieved in [13–15], we constructed various effective actions to describe the transitions at  $h_{c1}$  from the Z-x to the IC-SkX,  $h_{c2}$  in the middle of SOC  $\beta_1 < \beta < \beta_2$  from the Z-FM to the IC-SkX, then  $h_{c2}$  in the left of SOC  $0 < \beta < \beta_1$  from the Z-FM to the canted phase, finally from the canted to the IC-SkX at  $\beta_L$  to close the whole cycle in Fig.1. All the 4 effective actions reach consistent descriptions on the IC-SkX phase centered in the phase diagram. Our mean field analysis on these effective actions reproduced all the 5 ground states, the quantum fluctuations above the mean field reproduced all the excitations such as Goldstone, roton and Higgs modes above the ground states. Furthermore, we investigate the nature of all the 4 QPTs with the dynamic exponents  $z = 2$  single complex order parameter ( C-IC transition ),  $z = 2$  two complex order parameters ( C-IC ),  $z = 1$  one complex order parameter ( C-C ) and  $(z_x = 3/2, z_y = 3)$  ( C-IC ) with an order parameter fractionization from one to TWO complex order parameters.

We identify carefully the relation between the quantum spin and the order parameters in various effective actions. It is important in the following way:

(1) In the spinor boson case [22], the quantum spin is quadratically represented in terms of the two components complex order parameters  $\psi_1, \psi_2$ , it is the Zeeman field which directly tunes the relative magnitude between the two components. Here, near  $h = h_{c2}$ , there are also two components complex order parameters  $\psi_1, \psi_2$ , the Zeeman field  $h$  is implicitly embedded in the chemical potential term  $\mu = h_{c2} - h$ . Counter-intuitively, as shown in Sec.IV, the  $\psi_1, \psi_2$  always has equal amplitude, independent of the Zeeman field.

(2) The ratio of the quantum spins in A/B sublattice is determined by the two generalized Bogliubov matrix elements  $u, v$ . Even if getting to the  $\psi_{\pm}$  basis, it is always in the Ising limit where one of them vanishes, also independent of the Zeeman field. This is one of the crucial difference between the BEC of bosons and BEC of magnons: in the former, the quantum spin is quadratically represented in terms of the order parameter, in the latter, the quantum spin is linearly represented in terms of the order parameter, whose coefficients involve unitary transformation ( here below  $h_{c1}$  ) or Bogliubov transformation ( here above  $h_{c2}$  ). Even the two transformations are well defined only below  $h_{c1}$  or above  $h_{c2}$  respectively. The relation can be phenomenologically continued into  $h_{c1} < h < h_{c2}$  and match the microscopic SWE calculations.

(3) Although the universality classes of the transitions are completely determined by the order parameters, these relations are important to identify the correct spin-orbital orders of the states, also in evaluating the spin-spin correlation functions inside all the 5 phases, also near the QCP at a finite temperature which can be directly detected by all kinds of Bragg spectroscopy [32–37].

(4) There is an order parameter fractionization from one complex order parameter to two in the C-IC transition from canted to IC-SkX phase with the  $(z_x = 3/2, z_y = 3)$ . There is also a dynamic exponent change from  $z = 1$  to  $z = 2$ , Higgs mode to Roton mode. This fractionization is different than quantum spin fractionization into spinons plus a  $Z_2$  flux.

We also develop a new concept: Type-II dangerously irrelevant operators which considerably enrich the previously known Type-I dangerously irrelevant operators. It is instructive to look at the history associated with Type-II in different contexts: Type-II superconductors hosting a mixed vortex state in the presence of magnetic field was discovered after the Type-I superconductor. Type-II Weyl fermions [57] hosting a Fermi-surface with non-zero density of states was discovered after the Type-I Weyl points. More recently, Type-II OFQD hosting a nearly OFQD under a deformation was discovered after the Type-I OFQD which responses trivially under a deformation.

One can summarize the two different sources of the extra "doppler" shift term [49] in the Goldstone, roton or Higgs modes in Eq.13,31, 42.

(1) For IC-momentum, it is due to the Type-II dangerously irrelevant operators, the number of which is equal to the number of IC- momenta condensations: one  $V$  near  $h_{c1}$  for Eq.13 and two  $V_1, V_2$  near  $h_{c2}$  for Eq.31.

(2) For C-momentum, it is due to boosted term in the kinetic energy. This is the case for Eq.42. In fact, as shown in Sec.II and III, the effects of the dangerously irrelevant operators inside the symmetry broken IC-SkX phase can be transformed into the boosted form inside the kinetic energy.



The spin-spin correlation functions in Z-x phase is evaluated in the appendix D. It can similarly evaluated in all the other phases. The thermal conductivity  $\kappa_{xx}$  and Thermal Hall conductivity  $\kappa_{xy}$  in all the phases, especially in the QC regimes in Fig.1 and Fig.2 will also be studied in a separation publication [53].

The  $U(1)_{soc}$  symmetry only holds along the  $(\alpha = \pi/2, \beta)$  SOC line and the longitudinal Zeeman field. It may not hold in any general SOC systems. Here there could be many ways to break the  $U(1)_{soc}$  symmetry explicitly. One way is to apply a transverse field as discussed in appendix E. Another way is to look at a generic  $(\alpha, \beta)$ , or one can apply both at the same time. In [41], we studied various magnon condensations in a generic  $(\alpha, \beta)$  which has no  $U(1)_{soc}$  symmetry. As expected, it is quite different than the magnon condensation with the  $U(1)_{soc}$  symmetry addressed in this paper. Some crucial differences between the two were spelled out in the appendix F in [41]. It would be interesting to look at the phases and QPTs in Fig.1, especially the IC-SkX phase evolve Obviously, the Goldstone mode inside the canted phase and the IC-SkX phase will be gapped due to the explicit  $U(1)_{soc}$  symmetry breaking.

As mentioned at the end of Sec.VII, if extending the results to a honeycomb lattice with either bosons or fermions, the IC-SkX likely melts into a QSL, then the transitions at  $h_{c1}$  and  $h_{c2}$  will become two Topological transitions driven by the condensation of spinons or flux or some sort of fermions. Then it may be directly relevant to current trends searching for QSL driven by a Zeeman field in 4d or 5d Kitaev materials.

Recently, we also performed both microscopic and phenomenological effective actions to study Zeeman field induced quantum phase transitions of spinor bosons in the presence of  $\pi$  flux [20, 21] or in bosonic quantum Anomalous Hall systems [22]. Of course, the magnon condensations in the presence of SOC presented here with  $U(1)_{soc}$  and [41] without  $U(1)_{soc}$  is a different class of problems than the BEC in the presence of SOC in [20–22].

### Acknowledgements

We thank Dapeng Yu for hospitality during the authors visit at Institute for Quantum Science and Engineering, Shenzhen 518055, China. J.Ye thank Dr. Zhong Ruidan for experimental data related discussions.

## Appendix A: The relations of the symmetry operators between the previous works and the present

The RH model with generic  $0 < \beta < \alpha < \pi/2$  in the original basis is:

$$\mathcal{H} = -J \sum_i [S_i R_x(2\alpha) S_{i+x} + S_i R_y(2\beta) S_{i+y}] \quad (\text{A1})$$

Its symmetry are listed as [13–15, 41]

1. The Time reversal  $\mathcal{T} : S \rightarrow -S$  and  $k \rightarrow -k$  ( or equivalently  $(x, y) \rightarrow (x, y)$  ).
2. The translational symmetry:
3. The spin-orbital  $U(1)$  symmetry:
4. The three spin-orbital coupled  $Z_2$  symmetries [50]:

- (a)  $\tilde{\mathcal{P}}_x : (S^x, S^y, S^z) \rightarrow (S^x, -S^y, -S^z)$  and  $(k_x, k_y) \rightarrow (k_x, -k_y)$ ;
- (b)  $\tilde{\mathcal{P}}_y : (S^x, S^y, S^z) \rightarrow (-S^x, S^y, -S^z)$  and  $(k_x, k_y) \rightarrow (-k_x, k_y)$ ;
- (c)  $\tilde{\mathcal{P}}_z : (S^x, S^y, S^z) \rightarrow (-S^x, -S^y, S^z)$  and  $(k_x, k_y) \rightarrow (-k_x, -k_y)$ ;

The RH model with  $(\alpha = \pi/2, \beta)$  in a Zeeman field ( in the  $R_x(\pi/2)$ -rotated basis) is:

$$\mathcal{H} = -J \sum_i [S_i R_x(\pi) S_{i+x} + S_i R_z(2\beta) S_{i+y}] - H \sum_i S_i^z \quad (\text{A2})$$

whose symmetries are classified in [13–15] as:

1. The translational symmetry:
2. The spin-orbital  $U(1)$  symmetry:
3. The three spin-orbital coupled  $Z_2$  symmetries:
  - (a)  $\mathcal{T} \circ \tilde{\mathcal{P}}_x : (S^x, S^y, S^z) \rightarrow (-S^x, S^y, S^z)$  and  $(k_x, k_y) \rightarrow (-k_x, k_y)$  ( equivalently  $(x, y) \rightarrow (x, -y)$  ).
  - (b)  $\mathcal{T} \circ \tilde{\mathcal{P}}_y : (S^x, S^y, S^z) \rightarrow (S^x, -S^y, S^z)$  and  $(k_x, k_y) \rightarrow (k_x, k_y)$ ; ( equivalently  $(x, y) \rightarrow (-x, -y)$  ).

(c)  $\tilde{\mathcal{P}}_z : (S^x, S^y, S^z) \rightarrow (-S^x, -S^y, S^z)$  and  $(k_x, k_y) \rightarrow (-k_x, k_y)$ ;

4. The space reflection with respect to the y axis:  $\mathcal{I}_y : S \rightarrow S$  and  $(x, y) \rightarrow (-x, y)$  ( equivalently  $(k_x, k_y) \rightarrow (-k_x, k_y)$  ) which is the enlarged symmetry at  $\alpha = \pi/2$  absent at the generic  $(\alpha, \beta)$  discussed above. This enlarged symmetry at  $\alpha = \pi/2$  was missed in [13–15].

It is easy to see the following relations:  $\mathcal{T} \circ \tilde{\mathcal{P}}_x = \mathcal{T} \circ \mathcal{I}_x \circ \mathcal{P}_x$ ,  $\mathcal{T} \circ \tilde{\mathcal{P}}_y = \mathcal{T} \circ \mathcal{I}_x \circ \mathcal{I}_y \circ \mathcal{P}_y$ , and  $\mathcal{I}_y \circ \tilde{\mathcal{P}}_z = \mathcal{P}_z$ . In view of  $\mathcal{I}_y$  is conserved, the three spin-orbital coupled  $Z_2$  symmetries can be simplified as  $\mathcal{T} \circ \mathcal{I}_x \circ \mathcal{P}_x$ ,  $\mathcal{T} \circ \mathcal{I}_x \circ \mathcal{I}_y \circ \mathcal{P}_y$ ,  $\mathcal{P}_z$  which are identical to those listed in Sec.I.

## Appendix B: Spin-wave expansion to order $1/S$ .

We first review some results from spin-wave expansion (SWE) performed in [14]. Especially, we stress the unitary transformation in the Z-x state below  $h_{c1}$  and the FM state above  $h_{c2}$  which are crucial to derive the relations between the quantum spin and the order parameters inside the IC-SkX phase. As presented in Sec.II and III, the former is from bottom-up and the latter is from top-down.

### 1. Unitary transformation in the Z-x state in low field

In a weak magnetic field  $h < h_{c1}$ , the ground-state is the Z-x state with the classical spin configuration:

$$\mathbf{S}_i = S(0, 0, (-1)^{i_x}) \quad (\text{B1})$$

Performing the Holstein Primakoff transformation for A/B sublattice [14]

$$\begin{aligned} S_i^+ &= \sqrt{2S} \left( 1 - \frac{1}{2} \frac{n_i}{2S} + \dots \right) a_i, & S_i^- &= \sqrt{2S} a_i^\dagger \left( 1 - \frac{1}{2} \frac{n_i}{2S} + \dots \right), & S_i^z &= S - a_i^\dagger a_i, & i \in A; \\ S_j^+ &= \sqrt{2S} b_j^\dagger \left( 1 - \frac{1}{2} \frac{n_j}{2S} + \dots \right), & S_j^- &= \sqrt{2S} \left( 1 - \frac{1}{2} \frac{n_j}{2S} + \dots \right) b_j, & S_j^z &= -S + b_j^\dagger b_j, & j \in B. \end{aligned} \quad (\text{B2})$$

In momentum space, the Hamiltonian takes the form

$$\begin{aligned} \mathcal{H} &= -2NJS^2 + H \sum_k (a_k^\dagger a_k - b_k^\dagger b_k) + 4JS \sum_k (a_k^\dagger a_k + b_k^\dagger b_k) \\ &\quad - 2JS \sum_k [\cos k_x a_k^\dagger b_k + \cos k_x b_k^\dagger a_k + \cos(k_y - 2\beta) a_k^\dagger a_k + \cos(k_y + 2\beta) b_k^\dagger b_k] \end{aligned} \quad (\text{B3})$$

By performing a unitary transformation

$$a_{\mathbf{k}} = s_{\mathbf{k}} \alpha_{\mathbf{k}} + c_{\mathbf{k}} \beta_{\mathbf{k}}, \quad b_{\mathbf{k}} = s_{\mathbf{k}} \beta_{\mathbf{k}} - c_{\mathbf{k}} \alpha_{\mathbf{k}}, \quad (\text{B4})$$

where  $s_{\mathbf{k}} = \sin(\theta_{k,h}/2)$ ,  $c_{\mathbf{k}} = \cos(\theta_{k,h}/2)$ , and  $\tan \theta_{k,h} = \cos k_x / (\sin 2\beta \sin k_y - h)$ , the Hamiltonian can be put in the diagonal form:

$$\mathcal{H} = -2NJS^2 + 4JS \sum_k [\omega_+(k) \alpha_k^\dagger \alpha_k + \omega_-(k) \beta_k^\dagger \beta_k] \quad (\text{B5})$$

where the excitation spectrum is:

$$\omega_{\pm}(k) = 1 - \frac{1}{2} \cos 2\beta \cos k_y \pm \frac{1}{2} \sqrt{\cos^2 k_x + (\sin 2\beta \sin k_y - h)^2}. \quad (\text{B6})$$

The unitary transformation matrix elements  $s_{\mathbf{k}} = \sin(\theta_{k,h}/2)$  and  $c_{\mathbf{k}} = \cos(\theta_{k,h}/2)$  are useful to establish the connections between the quantum spin and the order parameter near  $h_{c1}$  in Eq.7.

## 2. Bogoliubov transformation in the FM in the high field

In a strong magnetic field, the ground-state is Z-FM state with the classical spin configuration:

$$\mathbf{S}_i = S(0, 0, 1) \quad (\text{B7})$$

Performing the standard Holstein Primakoff transformation

$$S_i^+ = \sqrt{2S} \left( 1 - \frac{1}{2} \frac{n_i}{2S} + \dots \right) a_i, \quad S_i^- = \sqrt{2S} a_i^\dagger \left( 1 - \frac{1}{2} \frac{n_i}{2S} + \dots \right), \quad S_i^z = S - a_i^\dagger a_i. \quad (\text{B8})$$

In momentum space, the Hamiltonian takes the form

$$\mathcal{H} = -NHS + H \sum_k a_k^\dagger a_k - JS \sum_k [2 \cos(k_y - 2\beta) a_k^\dagger a_k + \cos k_x (a_k a_{-k} + a_k^\dagger a_{-k}^\dagger)] \quad (\text{B9})$$

By introducing the Bogoliubov transformation as

$$a_{\mathbf{k}} = u_{\mathbf{k}} \alpha_{\mathbf{k}} + v_{\mathbf{k}} \alpha_{-\mathbf{k}}^\dagger, \quad a_{-\mathbf{k}}^\dagger = v_{\mathbf{k}} \alpha_{\mathbf{k}} + u_{\mathbf{k}} \alpha_{-\mathbf{k}}^\dagger. \quad (\text{B10})$$

where  $u_{\mathbf{k}} = \cosh \eta_k$ ,  $v_{\mathbf{k}} = \sinh \eta_k$  and  $\tanh 2\eta_k = \cos k_x / (h - \cos 2\beta \cos k_y)$ , the Hamiltonian takes the diagonal form

$$\begin{aligned} \mathcal{H} &= -NH(S + \frac{1}{2}) + JS \sum_k [\omega(k) \alpha_k^\dagger \alpha_k + \omega(-k) \alpha_{-k} \alpha_{-k}^\dagger] \\ &= -NH(S + \frac{1}{2}) + JS \sum_k \omega_k + 2JS \sum_k \omega_k \alpha_k^\dagger \alpha_k \end{aligned} \quad (\text{B11})$$

where the spin wave dispersion is

$$\omega_k = \sqrt{(h - \cos 2\beta \cos k_y)^2 - \cos^2 k_x - \sin 2\beta \sin k_y} \quad (\text{B12})$$

The Bogoliubov transformation matrix elements  $u_{\mathbf{k}}$  and  $v_{\mathbf{k}}$  are useful to establish the connections between the quantum spin and the order parameter near  $h_{c2}$  in Eq.26.

## Appendix C: Microscopic SWE calculations on the A/B sublattice ratio near $h_{c1}$ , $h_{c2}$ and $h_L$ .

In the classic limit ( $S \rightarrow \infty$ ), one can take the general ansatz of the IC-SkX state:

$$\begin{aligned} S_i &= S(\sin \theta_A \cos(\phi_A - k_0 i_y), \sin \theta_A \sin(\phi_A - k_0 i_y), \cos \theta_A), \quad i \in A \quad (i_x \text{ is odd}) \\ S_j &= S(\sin \theta_B \cos(\phi_B + k_0 j_y), \sin \theta_B \sin(\phi_B + k_0 j_y), \cos \theta_B), \quad j \in B \quad (j_x \text{ is even}) \end{aligned} \quad (\text{C1})$$

which is equivalent to:

$$\begin{aligned} S_i^z &= (S/2)[\cos \theta_A + \cos \theta_B + (-1)^{i_x}(\cos \theta_A - \cos \theta_B)] \\ S_i^+ &= (S/2)[\sin \theta_A + \sin \theta_B + (-1)^{i_x}(\sin \theta_A - \sin \theta_B)] e^{(-1)^{i_x} i(\phi_0 + k_0 i_y)} \end{aligned} \quad (\text{C2})$$

Then the ground-state energy is

$$E_{GS} = \min_{\theta_A, \theta_B, k_0} NJS^2 [\cos(\theta_A + \theta_B) + \sin^2(\beta + k_0/2) \sin^2 \theta_A + \sin^2(\beta - k_0/2) \sin^2 \theta_B - h(\cos \theta_A + \cos \theta_B) - 1] \quad (\text{C3})$$

The minimization procedure automatically gives  $\theta_A, \theta_B, k_0$  for the IC-SkX state which reduces to the FM state, canted state and Z-x state in the corresponding  $(\beta, h)$  regime.

Near  $h_{c2}$ , it gives  $\lim_{h \rightarrow h_{c2}^-} \theta_A = \lim_{h \rightarrow h_{c2}^-} \theta_B = 0$ , so Eq.C3 reduces to the Z-FM state with the non-trivial ratio:

$$\lim_{h \rightarrow h_{c2}^-} \frac{\sin \theta_A}{\sin \theta_B} = \lim_{h \rightarrow h_{c2}^-} \frac{h - \sqrt{3h^2 - 1 - h^4}}{h^2 - 1} = \sqrt{\sin^4 2\beta + \sin^2 2\beta} - \sqrt{\sin^4 2\beta - \cos^2 2\beta} \quad (\text{C4})$$

which matches Eq.C4 achieved by the effective action from  $h_{c2}^+$ .

thus it is easy to verify

$$\lim_{h \rightarrow h_{c2}^-} \frac{\sin \theta_A}{\sin \theta_B} \Big|_{\beta=\beta_1} = 1, \quad \lim_{h \rightarrow h_{c2}^-} \frac{\sin \theta_A}{\sin \theta_B} \Big|_{\beta=\pi/4} = \sqrt{2} - 1, \quad (C5)$$

Near  $h_{c1}$ , it gives  $\lim_{h \rightarrow h_{c1}^+} \theta_A = 0$ ,  $\lim_{h \rightarrow h_{c1}^+} \theta_B = \pi$ , so Eq.C3 reduces to the Z-x state with the non-trivial ratio:

$$\lim_{h \rightarrow h_{c1}^+} \frac{\sin \theta_A}{\sin \theta_B} = \lim_{h \rightarrow h_{c1}^+} [2 - \cos 2\beta \cos k_0 - \sqrt{(2 - \cos 2\beta \cos k_0)^2 - 1}] \quad (C6)$$

which matches Eq.8 achieved by the effective action from  $h_{c1}^-$ .

thus it is easy to verify

$$\lim_{h \rightarrow h_{c1}^+} \frac{\sin \theta_A}{\sin \theta_B} \Big|_{\beta=0} = 1, \quad \lim_{h \rightarrow h_{c1}^+} \frac{\sin \theta_A}{\sin \theta_B} \Big|_{\beta=\pi/4} = 2 - \sqrt{3}, \quad (C7)$$

The Ic-momentum along  $h_{c2}$  is found to be:

$$k_0 = \arccos[\cot 2\beta \sqrt{1 + \sin^2 2\beta}] \sim [40(\sqrt{5} - 1)]^{1/4} \sqrt{\beta - \beta_1} \quad (C8)$$

where the second equation works near  $\beta_1$ .

Near  $\beta_L$ , Eq.C3 reduces to the canted state with the non-trivial ratio:

$$\frac{\sin \theta_A}{\sin \theta_B} = 1 - \frac{\sin k_0}{\tan 2\beta_L} + O(k_0^2) \quad (C9)$$

At  $h = 1$ ,  $\cos 2\beta_L$  is root of equation  $z^4 + z^3 + 2z - 2 = 0$ .

#### Appendix D: The spin-spin correlation functions in the Z-x state below $h_{c1}$

Using the relations between the quantum spin and the order parameters, one can evaluate the spin-spin correlations functions in all the phases from the effective actions, especially their scaling functions near the QCPs. Here, for simplicity, we just evaluate them in the Z-x state.

The low-energy effective action corresponding to the Hamiltonian Eq.B5 can be written as

$$S_{\text{eff}} = \int_0^\beta d\tau \sum_k [\beta_{k,\tau}^* \partial_\tau \beta_{k,\tau} + 4JS\omega_{h,k}^- \beta_{k,\tau}^* \beta_{k,\tau}] = \sum_{k,\omega_n} [-i\omega_n + 4JS\omega_{h,k}^-] \beta^*(k, i\omega_n) \beta(k, i\omega_n) \quad (D1)$$

which leads to the only non-vanishing correlation function:

$$\chi_{\beta\beta^*}(k, i\omega_n) = \langle \beta(k, i\omega_n) \beta^*(k, i\omega_n) \rangle = \frac{1}{-i\omega_n + 4JS\omega_{h,k}^-} \quad (D2)$$

The relation between the quantum spin and the order parameter Eq.4 (or Eq.7) leads to

$$\langle S_A^+(k, i\omega_n) S_A^-(k, i\omega_n) \rangle = \langle S_B^-(k, i\omega_n) S_B^+(k, i\omega_n) \rangle = S(1 + \cos \theta_0) \langle \beta(k, i\omega_n) \beta^*(k, i\omega_n) \rangle \quad (D3)$$

and

$$\langle S_B^-(k, i\omega_n) S_A^-(k, i\omega_n) \rangle = \langle S_A^+(k, i\omega_n) S_B^+(k, i\omega_n) \rangle = S \sin \theta_0 \langle \beta(k, i\omega_n) \beta^*(k, i\omega_n) \rangle \quad (D4)$$

where  $\theta_{h,k} = \theta_{h,k=Q} = \theta_0$  are evaluated at the minimal  $\mathbf{K}_0 = (0, k_0)$ .

The analytical continuation of Eq.D2 leads to

$$\text{Im}[\chi_{\beta\beta^*}(k, i\omega_n \rightarrow \omega + i0^+)] = \pi \delta(4JS\omega_{h,k}^- - \omega) \quad (D5)$$

which leads to the equal-time correlation function by the fluctuation-dissipation theorem:

$$S_{\beta\beta^*}(k) = \int \frac{d\omega}{2\pi} \frac{-2\text{Im}[\chi_{\beta\beta^*}(k, \omega)]}{1 - e^{-\omega/T}} = 1 - \frac{1}{e^{4JS\omega_{h,k}^-/T} - 1} \quad (D6)$$

which leads to the equal-time SSCFs ( or structure factor ):

$$\begin{aligned} S_{AA}^{+-}(k) &= S_{BB}^{-+}(k) = S(1 + \cos \theta_0) \left[ 1 - \frac{1}{e^{4JS\omega_{h,k}^-/T} - 1} \right] \\ S_{AB}^{++}(k) &= S_{BA}^{--}(k) = S \sin \theta_0 \left[ 1 - \frac{1}{e^{4JS\omega_{h,k}^-/T} - 1} \right] \end{aligned} \quad (\text{D7})$$

Following [13], one can define the uniform spin  $M = (S_A + S_B)/2$  and the staggered spin  $M = S_A - S_B$ , then

$$\begin{aligned} S_u^{+-}(k) &= \frac{1}{4} S_{AA}^{+-}(k) = \frac{1}{2} S \cos^2(\theta_0/2) \left[ 1 - \frac{1}{e^{4JS\omega_{h,k}^-/T} - 1} \right] \\ S_u^{++}(k) &= -S_{AB}^{++}(k) = -S \sin \theta_0 \left[ 1 - \frac{1}{e^{4JS\omega_{h,k}^-/T} - 1} \right] \end{aligned} \quad (\text{D8})$$

which, after exchanging the order of the spin operators, match those achieved in [13] by the spin wave expansion.

For a generic  $(\alpha, \beta)$  in Eq.1 which breaks the  $U(1)_{\text{soc}}$  explicitly, identifying the low energy modes is much more involved, so evaluating the spin-spin correlation functions is much more involved in [41].

### Appendix E: Order parameter and the QPT in the transverse fields

As mentioned in the introduction, due to the SOC, the response to a Zeeman field depends on the orientation of the field. Here, we apply a transverse field [15] to the RFHM in Eq.M1:

$$\mathcal{H} = \mathcal{H}_{\text{RH}} - \mathbf{H} \cdot \sum_i \mathbf{S}_i. \quad (\text{E1})$$

where the two transverse fields are  $\mathbf{H} \parallel \hat{x}$  or  $\mathbf{H} \parallel \hat{y}$ . Both break the  $U(1)_{\text{soc}}$ . So it should be quite different than the case with  $U(1)_{\text{soc}}$ . Indeed, as shown in [15], in contrast to the longitudinal case [14], the C- magnons always emerge out in the competition against the IC- magnons and drive the QPT. The magnon condensation by the SWE in [15] suggests the order parameter takes the form:

$$\langle \alpha_{\mathbf{k}} \rangle = \psi \delta_{\mathbf{k}, \mathbf{Q}} \quad (\text{E2})$$

where  $\mathbf{Q} = (\pi, 0)$  is the C- condensation momentum.

This type of magnon condensation leads to the transverse spin components:

$$\begin{aligned} \langle S_i^z + iS_i^y \rangle &\propto (-1)^{i_x} (u\psi + v\psi^*) \propto (-1)^{i_x} (\psi + \psi^*), \text{ for } \mathbf{H} \parallel \hat{x} \\ \langle S_i^z + iS_i^x \rangle &\propto (-1)^{i_x} (u\psi + v\psi^*) \propto (-1)^{i_x} (\psi + \psi^*), \text{ for } \mathbf{H} \parallel \hat{y} \end{aligned} \quad (\text{E3})$$

where, as alerted in Sec.IV,  $u = u_{\mathbf{Q}} = \infty$  and  $v = v_{\mathbf{Q}} = \infty$ , but  $u/v = 1$ , so can be simply factored out in the relation between the quantum spin and the order parameter. The above equation suggests the order parameter can be taken as one REAL field  $\phi = \psi + \psi^*$ .

The symmetry of the Hamiltonian  $\mathcal{H}$  in  $H_x$  is generated by 1) translation  $\mathcal{T}_x$  and  $\mathcal{T}_y$ ; 2) space reflection  $\mathcal{I}_y$ ; 3) spin-orbital reflection  $\mathcal{I}_x \circ \mathcal{P}_x$ ,  $\mathcal{T} \circ \mathcal{I}_x \circ \mathcal{P}_y$ ,  $\mathcal{T} \circ \mathcal{P}_z$ . The translation takes  $\phi(x, y) \rightarrow \phi(x, y)$ , and space reflection  $\mathcal{I}_y$  takes  $\phi(x, y) \rightarrow \phi(-x, y)$ , but spin-orbital reflection  $\mathcal{I}_x \circ \mathcal{P}_x : \phi(x, y) \rightarrow -\phi(x, -y)$ ,  $\mathcal{T} \circ \mathcal{I}_x \circ \mathcal{P}_y : \phi(x, y) \rightarrow \phi(x, -y)$ ,  $\mathcal{T} \circ \mathcal{P}_z : \phi(x, y) \rightarrow -\phi(x, y)$ .

The symmetry of the Hamiltonian  $\mathcal{H}$  in  $H_y$  has the same 1) and 2), but 3) spin-orbital reflections become  $\mathcal{I}_x \circ \mathcal{P}_y$ ,  $\mathcal{T} \circ \mathcal{I}_x \circ \mathcal{P}_x$ ,  $\mathcal{T} \circ \mathcal{P}_z$ . The translation takes  $\phi(x, y) \rightarrow \phi(x, y)$ , and space reflection  $\mathcal{I}_y$  takes  $\phi(x, y) \rightarrow \phi(-x, y)$ , but spin-orbital reflection  $\mathcal{I}_x \circ \mathcal{P}_y : \phi(x, y) \rightarrow -\phi(x, -y)$ ,  $\mathcal{T} \circ \mathcal{I}_x \circ \mathcal{P}_x : \phi(x, y) \rightarrow \phi(x, -y)$ ,  $\mathcal{T} \circ \mathcal{P}_z : \phi(x, y) \rightarrow -\phi(x, y)$ .

Obviously, the high field X-FM or Y-FM state breaks no symmetries of the corresponding Hamiltonian. So the above analysis leads to the effective action with  $z = 1$ :

$$\mathcal{S} = \int d\tau d^2r [(\partial_\tau \phi)^2 + v_x^2 (\partial_x \phi)^2 + v_y^2 (\partial_y \phi)^2 - \mu \phi^2 + u \phi^4] \quad (\text{E4})$$

where  $\phi$  is a real scalar field and the SWE in [15] shows  $\mu = h_c - h$ . Note that the spin-orbital  $Z_2$  reflection, i.e.  $\mathcal{T} \circ \mathcal{P}_z : \phi \rightarrow -\phi$  dictates the absence of odd power of  $\phi$  terms. This is nothing but standard 3D Ising universality class.

At mean field level,  $\psi = m$

$$\mathcal{S}_0 = -\mu m^2 + um^4 \quad (\text{E5})$$

When  $\mu = h_c - h < 0$ ,  $m = 0$ , which means the fully polarized spin state  $\langle \mathbf{S}_i \rangle = S(1, 0, 0)$  for  $\mathbf{H} \parallel \hat{x}$  and  $\langle \mathbf{S}_i \rangle = S(0, 1, 0)$  for  $\mathbf{H} \parallel \hat{y}$ . When  $\mu > 0$ ,  $m^2 = \mu/2u$ , which means the canted phase  $\langle \mathbf{S}_i \rangle = (\sqrt{S^2 - m^2}, 0, (-1)^{i_x} m)$  for  $\mathbf{H} \parallel \hat{x}$  and  $\langle \mathbf{S}_i \rangle = (0, \sqrt{S^2 - m^2}, (-1)^{i_y} m)$  for  $\mathbf{H} \parallel \hat{y}$ .

When  $\mu < 0$ , the action to the quadratic order:

$$\mathcal{S}_2 = \int d\tau d^2r [(\partial_\tau \phi)^2 + v_x^2 (\partial_x \phi)^2 + v_y^2 (\partial_y \phi)^2 - \mu \phi^2] \implies \omega_k = \sqrt{-\mu + v_x^2 k_x^2 + v_y^2 k_y^2} \quad (\text{E6})$$

which coincides with the spectrum inside the FM phase achieved by SWE in [15].

When  $\mu > 0$ , expanding  $\phi = m + \delta\phi$  to the quadratic order

$$\mathcal{S}_2 = \int d\tau d^2r [(\partial_\tau \delta\phi)^2 + v_x^2 (\partial_x \delta\phi)^2 + v_y^2 (\partial_y \delta\phi)^2 + (6m^2 u - \mu) \delta\phi^2] \implies \omega_k = \sqrt{(6m^2 u - \mu) + v_x^2 k_x^2 + v_y^2 k_y^2} \quad (\text{E7})$$

which may also be rewritten as  $\omega_k = \sqrt{2\mu + v_x^2 k_x^2 + v_y^2 k_y^2}$ . It coincides with the spectrum inside the canted phase achieved by SWE in [15].

It is easy to show that the QPTs at the special Abelian points in the two transverse field cases is similar as that in the longitudinal case studied in the main text, so it is in the 3d XY universality class.

The generic  $(\alpha, \beta)$  case also breaks the  $U(1)_{\text{soc}}$  symmetry explicitly and the order parameter is also real [41]. However, in contrast to the transverse field case where only C-magnon condensations can happen, there are both C- and IC-magnons condensations which lead to different QPTs in [41].

## Appendix F: Order parameter and the QPT of the AFM in a uniform field

For an AFM in a uniform field, a big  $h$  leads to a fully polarized state, Z-FM state, which is not only the ground state but also an exact eigenstate. A Simple spin-wave calculation shows  $\omega \sim \Delta + v^2 k^2$  near  $(\pi, \pi)$ . In this case, because it is an exact eigenstate, neither Bogoliubov transformation nor unitary transformation is needed, thus the relation between the spin and the order parameter is simply  $\langle S_i^+ \rangle = (-1)^{i_x + i_y} \psi$  with a complex field  $\psi$ . The effective action consistent with the  $U(1)_s$  symmetry has  $z = 2$ :

$$\mathcal{S} = \int d\tau d^2r [\psi^* \partial_\tau \psi + v^2 |\nabla \psi|^2 - \mu |\psi|^2 + U |\psi|^4] \quad (\text{F1})$$

which belongs to  $z = 2$  zero density SF-Mott transition universality class, therefore confirm the assumption used in [19].

When  $\mu < 0$ ,  $\psi = 0$  the mean field ground state is Z-FM state. While  $\mu > 0$ ,  $\psi = me^{i\phi_0}$  the mean field ground state is canted state

$$\mathbf{S}_i = ((-1)^{i_x + i_y} m \cos \phi_0, (-1)^{i_x + i_y} m \sin \phi_0, \sqrt{S^2 - m^2})$$

As mentioned in Sec.IV-C and also appendix E, at the Abelian point  $\beta = 0$ ,  $c = 0$  in Eq.35, the Hamiltonian has an additional space reflection with respect to  $x$  axis, thus  $c = 0$  belongs to standard 3D XY universality class with the dynamic exponent  $z = 1$  which is dramatically different than the above case.

- 
- [1] M. Z. Hasan and C. L. Kane, *Colloquium: Topological insulators*, Rev. Mod. Phys. **82**, 3045 (2010).
  - [2] X. L. Qi and S. C. Zhang, *Topological insulators and superconductors*, Rev. Mod. Phys. **83**, 1057 (2011).
  - [3] L. Savary and L. Balents, *Quantum Spin liquids*, arXiv:1601.03742 (2016).
  - [4] C. Broholm, R. J. Cava, S. A. Kivelson, D. G. Nocera, M. R. Norman, T. Senthil, Quantum spin liquids, Science 17 Jan 2020: Vol. 367, Issue 6475, eaay0668, DOI: 10.1126/science.aay0668
  - [5] Y. J. Lin, R. L. Compton, A. R. Perry, W. D. Phillips, J. V. Porto, and I. B. Spielman, Phys. Rev. Lett. 102, 130401 (2009); Y. J. Lin, R. L. Compton, K. Jimnez-Garcia, J. V. Porto, and I. B. Spielman, Nature (London) 462, 628 (2009); Y. J. Lin, R. L. Compton, K. Jimnez-Garcia, W. D. Phillips, J. V. Porto, and I. B. Spielman, Nat. Phys. 7, 531 (2011); Y.-J. Lin, K. Jimnez-Garcia, and I. B. Spielman, Nature (London) 471, 83 (2011).

- [6] Pengjun Wang, Zeng-Qiang Yu, Zhengkun Fu, Jiao Miao, Lianghai Huang, Shijie Chai, Hui Zhai and Jing Zhang, Spin-Orbit Coupled Degenerate Fermi Gases, *Phys. Rev. Lett.* 109, 095301 (2012).
- [7] Jin-Yi Zhang, Si-Cong Ji, Zhu Chen, Long Zhang, Zhi-Dong Du, Bo Yan, Ge-Sheng Pan, Bo Zhao, You-Jin Deng, Hui Zhai, Shuai Chen, and Jian-Wei Pan, Collective Dipole Oscillations of a Spin-Orbit Coupled Bose-Einstein Condensate, *Phys. Rev. Lett.* 109, 115301 (2012).
- [8] Lianghai Huang, *et.al*, Experimental realization of a two-dimensional synthetic spin-orbit coupling in ultracold Fermi gases, *Nature Physics* 12, 540-544 (2016).
- [9] Zengming Meng, *et.al*, Experimental observation of topological band gap opening in ultracold Fermi gases with two-dimensional spin-orbit coupling, arXiv:1511.08492.
- [10] Michael L. Wall, *et.al*, Synthetic Spin-Orbit Coupling in an Optical Lattice Clock, *Phys. Rev. Lett.* 116, 035301 (2016).
- [11] Zhan Wu, *et.al*, Realization of Two-Dimensional Spin-orbit Coupling for Bose-Einstein Condensates, *Science* 354, 83-88 (2016).
- [12] Nathaniel Q. Burdick, Yijun Tang, and Benjamin L. Lev, Long-Lived Spin-Orbit-Coupled Degenerate Dipolar Fermi Gas, *Phys. Rev. X* 6, 031022 (2016).
- [13] Fadi Sun, Jinwu Ye, Wu-Ming Liu, Quantum magnetism of spinor bosons in optical lattices with synthetic non-Abelian gauge fields at zero and finite temperatures, *Phys. Rev. A* 92, 043609 (2015).
- [14] Fadi Sun, Jinwu Ye, Wu-Ming Liu, Quantum incommensurate skyrmion crystals and commensurate to in-commensurate transitions in cold atoms and materials with spinorbit couplings in a Zeeman field, *New J. Phys.* 19, 083015 (2017). In the microscopic SWE in this work, the authors only considered the dispersion relation in the quantum Lifshitz transition from the canted phase to the IC-SkX, lead to an in-correct dynamic exponents  $z = (1, 3)$ . By considering the full effective action Eq.49, we find the correct  $z = (3/2, 3)$ . Also the SWE in this work can not distinguish what is the physical mechanism of the gapped "roton" mode. Only when only working out the effective action Eq.35 with  $z = 1$ , one can identify the "roton" mode Eq.42 inside the canted phase is, in fact, a Higgs mode. Similarly, only when only working out the effective action Eq.16, 18 or Eq.21 with  $z = 2$ , one can identify the "roton" mode Eq.31 inside the IC-SkX phase is a true roton mode.
- [15] Fadi Sun, Jinwu Ye, Wu-Ming Liu, Classification of magnons in Rotated Ferromagnetic Heisenberg model and their competing responses in transverse fields, *Phys. Rev. B* 94, 024409 (2016).
- [16] A. V. Chubukov, S. Sachdev, and J. Ye, *Theory of two-dimensional quantum Heisenberg antiferromagnets with a nearly critical ground state*, *Phys. Rev. B* 49, 11919(1994).
- [17] S. Sachdev, *Quantum Phase transitions*, (2nd edition, Cambridge University Press, 2011).
- [18] A. Auerbach, *Interacting electrons and quantum magnetism*, (Springer Science & Business Media, 1994).
- [19] Subir Sachdev, T. Senthil, and R. Shankar, Finite-temperature properties of quantum antiferromagnets in a uniform magnetic field in one and two dimensions, *Phys. Rev. B* 50, 258 (1994).
- [20] Fadi Sun and Jinwu Ye, Goldstone modes generated by order from quantum disorder and its experimental observation, arXiv:1711.06304, substantially revised version No.2.
- [21] Fadi Sun and Jinwu Ye, Quantum spin liquids in a square lattice subject to an Abelian flux and its experimental observation, arXiv:2005.04695.
- [22] Fadi Sun and Jinwu Ye, Nearly order from quantum disorder phenomena (NOFQD): its application and detection in the bosonic quantum anomalous Hall system, arXiv:1903.11134, substantially revised version No.2.
- [23] Fadi Sun, Junsen Wang, Jinwu Ye and Youjin Deng, Frustrated superfluids, their transitions to Y-x Mott state and quantum spin liquids in a non-Abelian flux, arXiv:1712.06545, substantially revised version 2 to be put in arXiv soon.
- [24] Fadi Sun, Junsen Wang, Jinwu Ye and Youjin Deng, Global phase diagram of Quantum Anomalous Hall system of spinor bosons in a square lattice: spin-bond correlated superfluids, Mott states and quantum spin liquids, arXiv:1711.11580, substantially revised version 2 to be put in arXiv soon.
- [25] Here when classifying the symmetries, we use a slightly different notation than that used in the previous works [13–15, 58]. The only symmetry not realized is the space reflection with respect to  $y$  axis  $\mathcal{I}_y$ . See appendix A for details.
- [26] The in-commensurate is always important in SOC systems, for example, it leads to the gapless 1d Luttinger liquids embedded in 2d in [41]. It also leads to dramatic effects in spinor bosons condensing at in-commensurate momenta [23, 24].
- [27] Note that our microscopic calculations in [14] also find more higher derivative terms such as  $v_{xx}(\partial_x^2 \phi)^2 + v_{yy}(\partial_y^2 \phi)^2 + v_{xy}\partial_x^2 \phi \partial_y^2 \phi$ , but including these extra terms will not change the results derived in the following, so we will not write them out explicitly.
- [28] The effective action Eq.21 can be contrasted with that in [22] to describe the quantum phase transition induced by a Zeeman field due to the nearly order from quantum disorder (NOFQD) phenomenon.
- [29] D. S. Rokhsar and S. A. Kivelson, *Superconductivity and the Quantum Hard-Core Dimer Gas*, *Phys. Rev. Lett.* 61, 2376 (1988).
- [30] Eduardo Fradkin, David A. Huse, R. Moessner, V. Oganesyan, and S. L. Sondhi, Bipartite RokhsarKivelson points and Cantor deconfinement, *Phys. Rev. B* 69, 224415 (2004)
- [31] Ashvin Vishwanath, L. Balents, and T. Senthil, Quantum criticality and deconfinement in phase transitions between valence bond solids *Phys. Rev. B* 69, 224416 (2004).
- [32] J. Ye, J. M. Zhang, W. M. Liu, K. Zhang, Y. Li, and W. Zhang *Light-scattering detection of quantum phases of ultracold atoms in optical lattices*, *Phys. Rev. A* 83, 051604 (2011); J. Ye, K. Y. Zhang, Y. Li, Y. Chen, and W. P. Zhang, *Optical Bragg, atom Bragg and cavity QED detections of quantum phases and excitation spectra of ultracold atoms in bipartite and frustrated optical lattices*, *Ann. Phys.* 328, 103 (2013).
- [33] M. Kozuma, *et.al*, Coherent Splitting of Bose-Einstein Condensed Atoms with Optically Induced Bragg Diffraction, *Phys. Rev. Lett.* 82, 871 (1999); J. Stenger, *et al*, Bragg Spectroscopy of a Bose-Einstein Condensate, *Phys. Rev. Lett.* 82, 4569

- (1999); D. M. Stamper-Kurn *et al*, Excitation of Phonons in a Bose-Einstein Condensate by Light Scattering, Phys. Rev. Lett. 83, 2876 - 2879 (1999); J. Steinhauer, *et.al*, Phys. Rev. Lett. 88, Excitation Spectrum of a Bose-Einstein Condensate, 120407, (2002); S. B. Papp, *et.al*, Bragg Spectroscopy of a Strongly Interacting Rb 85 Bose-Einstein Condensate, Phys. Rev. Lett. 101, 135301 (2008)
- [34] P. T. Ernst, *et al*, Probing superfluids in optical lattices by momentum-resolved Bragg spectroscopy, Nature Physics 6, 56 (2010 ).
- [35] T. Stoferle *et al*, Transition from a Strongly Interacting 1D Superfluid to a Mott Insulator, Phys. Rev. Lett. 92, 130403 (2004).
- [36] G. Birkel, *et al*, Bragg Scattering from Atoms in Optical Lattices, Phys. Rev. Lett. 75, 2823 (1995); M. Weidemüller, *et al*, Bragg Diffraction in an Atomic Lattice Bound by Light, Phys. Rev. Lett. 75, 4583 (1995), Local and global properties of light-bound atomic lattices investigated by Bragg diffraction, Phys. Rev. A 58, 4647 (1998). J. Ruostekoski, C. J. Foot, and A. B. Deb, Light Scattering for Thermometry of Fermionic Atoms in an Optical Lattice, Phys. Rev. Lett. 103, 170404 (2009).
- [37] Si-Cong Ji, Long Zhang, Xiao-Tian Xu, Zhan Wu, Youjin Deng, Shuai Chen, Jian-Wei Pan, Softening of Roton and Phonon Modes in a Bose-Einstein Condensate with Spin-Orbit Coupling, Phys. Rev. Lett. 114, 105301 (2015).
- [38] For scaling functions with the anisotropic dynamic exponents ( $z_x = 2, z_y = 1$ ) where  $q_x$  is the colliding direction across a fermionic Lifshitz type of transitions, see F. Sun, X.-L. Yu, J. Ye, H. Fan, and W.-M. Liu, *Topological Quantum Phase Transition in Synthetic Non-Abelian Gauge Potential: Gauge Invariance and Experimental Detections*, Sci. Rep. 3, 2119 (2013).
- [39] X. Z. Yu, Y. Onose, N. Kanazawa, J. H. Park, J. H. Han, Y. Matsui, N. Nagaosa and Y. Tokura, Real-space observation of a two-dimensional skyrmion crystal, Nature 465, 901904 (17 June 2010).
- [40] Ye, J. Duality, magnetic space group and their applications to quantum phases and phase transitions on bipartite lattices in several experimental systems. *Nucl. Phys. B* 805, 418 (2008).
- [41] Fadi Sun and Jinwu Ye, Complete, in-complete devil staircases and Luttinger Liquids Cantor set of strongly interacting spin-orbit coupled bosons in a lattice, arXiv:1603.00451, substantially revised version 3 submitted to Phys. Rev. X
- [42] Jinwu Ye, Elementary excitations in a supersolid, Europhysics Letters, 82 (2008) 16001
- [43] Jinwu Ye, Quantum Phases of Excitons and Their Detections in Electron-Hole Semiconductor Bilayer Systems, J. Low Temp Phys. 158(5), 882-900 (2010).
- [44] Jinwu Ye, Elementary excitations, Spectral weights and Experimental signatures of a Supersolid and Larkin-Ovchinnikov-Fulde - Ferrell (LOFF) state, J. Low Temp Phys. 160(3), 71-111, (2010)
- [45] Yu Chen, Jinwu Ye and Quang Shan Tian, Classification of a supersolid: Symmetry breaking and Excitation spectra, Journal of Low Temperature Physics: 169 (2012), 149-168.
- [46] In fact, one may intend to add a  $B(|\psi_1|^2 - |\psi_2|^2)^2$  term. However, under  $U(1)_{\text{soc}}$ , it changes as  $(|\psi_1|^2 - |\psi_2|^2)^2 = (\psi_+ \psi_-^* + \psi_+^* \psi_-)^2 \rightarrow (e^{+2i\phi_0} \psi_+ \psi_-^* + e^{-2i\phi_0} \psi_+^* \psi_-)^2 = \cos^2(2\phi_0)(\psi_+ \psi_-^* + \psi_+^* \psi_-)^2 + \sin^2(2\phi_0)(\psi_+ \psi_-^* - \psi_+^* \psi_-)^2$ . So this term is absent in the effective action.
- [47] For Goldstone and Higgs modes inside a cavity, see Yu Yi-Xiang, Jinwu Ye and W.M. Liu, Goldstone and Higgs modes of photons inside an cavity and their detections, Scientific Reports 3, 3476 (2013).
- [48] There maybe some common insights shared between the symmetry breaking analysis and finite temperature phase transitions in this paper and those in: Shang-Shun Zhang, Jinwu Ye, Wu-Ming Liu, Itinerant magnetic phases and Quantum Lifshitz transitions in repulsively interacting spin-orbit coupled Fermi gas, Phys. Rev. B 94, 115121 (2016).
- [49] In high temperature superconductors, the fermionic quasi-particle spectrum also acquires such an extra doppler shift term due to the superflow of a vortex far away. See Jinwu Ye, Random magnetics fields and the quasi-particle transports in the mixed state of high  $T_c$  cuprates, Phys. Rev. Lett. 86, 316 (2001). Jinwu Ye, Thermally generated vortices, gauge invariance and electron spectral function in the pseudo-gap regime, Phys. Rev. Lett. 87, 227003 (2001).
- [50] The original  $\mathcal{P}$  in [13–15, 41] is denoted by  $\bar{\mathcal{P}}$  here.
- [51] Similar situations happen also in the spinor bosons, see appendix C of [22].
- [52] A. Kitaev, Anyons in an exactly solved model and beyond. Ann. Phys. 321, 2111 (2006). doi: 10.1016/j.aop.2005.10.005
- [53] Fadi Sun and Jinwu Ye, in preparation.
- [54] Y. Kasahara, T. Ohnishi, Y. Mizukami, O. Tanaka, Sixiao Ma, K. Sugii, N. Kurita, H. Tanaka, J. Nasu, Y. Motome, T. Shibauchi, Y. Matsuda, Majorana quantization and half-integer thermal quantum Hall effect in a Kitaev spin liquid, Nature 559, 227-231 (2018).
- [55] Y. Kasahara, K. Sugii, T. Ohnishi, M. Shimozawa, M. Yamashita, N. Kurita, H. Tanaka, J. Nasu, Y. Motome, T. Shibauchi, and Y. Matsuda, Unusual Thermal Hall Effect in a Kitaev Spin Liquid Candidate  $\alpha - \text{RuCl}_3$ , Phys. Rev. Lett. 120, 217205 Published 25 May 2018.
- [56] Yanting Teng, Yunchao Zhang, Rhine Samajdar, Mathias S. Scheurer, Subir Sachdev, Unquantized thermal Hall effect in quantum spin liquids with spinon Fermi surfaces, Phys. Rev. Research 2, 033283 (2020). See also all the references cited in this work on current theoretical and experimental status on searching for quantum spin liquids in 4d or 5d Kitaev materials.
- [57] Fadi Sun and Jinwu Ye, Type I and Type II fermions, Topological depletions and sub-leading scalings across topological phase transitions, Phys. Rev. B 96, 035113 (2017).
- [58] Fadi Sun, Jinwu Ye, Wu-Ming Liu, Fermionic Hubbard model with Rashba or Dresselhaus spin-orbit coupling, New J. Phys. 19, 063025 (2017).
- [59] In the experiments [54, 55], there is very little anisotropy in the direction of the in-plane magnetic field, but dramatic



difference between the in-plane and c-axis. J.Ye thank Dr. Zhong Ruidan for alerting us this fact. Our case is extremely sensitive to the in-plane angle also due to the special  $U(1)_{soc}$ . After breaking the  $U(1)_{soc}$  symmetry explicitly, the sensitivity drops, but still depends on the in-plane angle. So it is not known how to interpretate the insensitivity of the in-plane angle in the two experiments.